Rismondo J, Wamp S, Aldridge C, Vollmer W, Halbedel S. Stimulation of PgdA-dependent peptidoglycan N-deacetylation by GpsB-PBP A1 in *Listeria monocytogenes*. *Molecular Microbiology* 2017

Stimulation of PgdA-dependent peptidoglycan N-deacetylation by GpsB-PBP A1 in *Listeria monocytogenes*

Jeanine Rismondo[1,2], Sabrina Wamp[1], Christine Aldridge[3,4], Waldemar Vollmer[3] and Sven Halbedel[1,*]

[1] FG11 Division of Enteropathogenic bacteria and *Legionella*, Robert Koch Institute, Burgstrasse 37, 38855 Wernigerode, Germany

[2] present address: Section of Microbiology and MRC Centre for Molecular Bacteriology and Infection, Imperial College London, London SW7 2AZ, United Kingdom

[3] Institute for Cell and Molecular Biosciences, The Centre for Bacterial Cell Biology, Newcastle University, Newcastle upon Tyne NE2 4AX, United Kingdom

[4] present address: School of Biomedical Sciences, Newcastle University, Newcastle upon Tyne NE2 4AX, United Kingdom

[*] Corresponding author:

halbedels@rki.de, Robert Koch Institute, FG11 Division of Enteropathogenic bacteria and Legionella, Burgstrasse 37, D-38855 Wernigerode, Germany; phone: +49-30-18754-4323; fax: +49-30-18754-4207;

Short title: *L. monocytogenes* peptidoglycan N-deacetylation

Keywords: peptidoglycan modification/ DivIVA proteins/ cell division / cell wall biosynthesis

ABSTRACT

Listeria monocytogenes and other pathogenic bacteria modify their peptidoglycan to protect it against enzymatic attack through the host innate immune system, such as the cell wall hydrolase lysozyme. During our studies on GpsB, a late cell division protein that controls activity of the bi-functional penicillin binding protein PBP A1, we discovered that GpsB influences lysozyme resistance of *L. monocytogenes*. Mutant strains lacking *gpsB* were prone to spontaneous autolysis but showed an increased lysozyme resistance. Deletion of *pbpA1* corrected this effect, demonstrating that PBP A1 is also involved in this. Susceptibility to lysozyme mainly depends on two peptidoglycan modifying enzymes: The peptidoglycan N-deacetylase PgdA and the peptidoglycan O-acetyltransferase OatA. Genetic and biochemical experiments consistently demonstrated that the increased lysozyme resistance of the Δ*gpsB* mutant was PgdA-dependent and OatA-independent. Protein-protein interaction studies supported the idea that GpsB, PBP A1 and PgdA form a complex in *L. monocytogenes* and identified the regions in PBP A1 and PgdA required for complex formation. These results establish a physiological connection between GpsB, PBP A1 and the peptidoglycan modifying enzyme PgdA. To our knowledge, this is the first reported link between a GpsB-like cell division protein and factors important for escape from the host immune system.

INTRODUCTION

The Gram-positive bacterium *L. monocytogenes* is a harmful human pathogen associated with frequent food-borne outbreaks of gastroenteritis. In certain risk groups, such as the elderly, pregnant women and neonates, listeriosis can develop into more systemic conditions, including septicemia, fetal infections in pregnant women, as well as meningitis, and such cases of invasive listeriosis have a high mortality rate of up to 30% (Allerberger & Wagner, 2010, Swaminathan & Gerner-Smidt, 2007). *L. monocytogenes* actively invades human host cells, multiplies inside their cytoplasm and spreads to neighboring cells, so that the bacterium effectively disseminates the surrounding tissue (Cossart & Toledo-Arana, 2008). Intracellular passages facilitate escape from the immune system, but also impair antibiotic therapy, since antibiotics have to penetrate the host cells in order to exert their anti-listerial effects (Hof, 2004). Another mechanism, which impairs efficient eradication of *L. monocytogenes* by the innate immune system is their high intrinsic resistance against the muramidase lysozyme (Warren *et al.*, 2015, Rae *et al.*, 2011), which is part of the unspecific humoral host defense against bacterial pathogens.

Resistance against cell wall hydrolysis by lysozyme is mediated by two peptidoglycan (PG) modifications in *L. monocytogenes*. First, N-acetylglucosamine residues (GlcNAc) are deacetylated by PgdA, and second, N-acetylmuramic acid (MurNAc) residues are acetylated by the O-acetyltransferase OatA (Boneca *et al.*, 2007, Aubry *et al.*, 2011). Roughly 50% of all GlcNAc residues are deacetylated, whereas approximately 23% of all MurNAc residues are acetylated at their C_6-OH (Boneca *et al.*, 2007, Aubry *et al.*, 2011). Both modifications turn peptidoglycan into a poor substrate for lysozyme on their own (Vollmer, 2008), but the combination of both results in a synergistic increase of lysozyme resistance (Rae *et al.*, 2011). PgdA is predicted to be a membrane protein with one transmembrane domain, whereas OatA is a

multi-spanning membrane-integral protein with its enzymatic domain exposed to the extracellular space. It is currently not known, whether both proteins are associated with the PG chain polymerizing penicillin binding proteins (PBPs) or whether they act independently from this process. A recent transposon mutagenesis study has identified further determinants of lysozyme resistance of *L. monocytogenes* (Burke *et al.*, 2014). Among these were the response regulator DegU and the regulatory small RNA *rli31*, both of which are required for full expression of *pgdA*. PbpX, encoding a putative β-lactamase, was also identified in this screen, but how PbpX contributes to lysozyme resistance is still not known (Burke *et al.*, 2014).

We are interested in control of cell growth and division by GpsB proteins. GpsB is a membrane-associated, cytoplasmic protein that accumulates at the cell division sites (Claessen *et al.*, 2008, Tavares *et al.*, 2008). *L. monocytogenes* GpsB interacts with penicillin binding protein A1 via a conserved surface exposed patch in its N-terminal domain and is crucial to control activity of this protein (Rismondo *et al.*, 2016). Deletion of *gpsB* caused heat-sensitive growth, defects in cell division and increased sensitivity against cell wall-active compounds such as penicillin, indicating distortions in cell wall biosynthesis (Rismondo *et al.*, 2016). These observations are explained by uncoordinated activity of PBP A1 in the absence of GpsB, since deletion of *pbpA1* partially suppressed several of the Δ*gpsB* phenotypes (Rismondo *et al.*, 2016).

GpsB is a tripod-like hexamer with three DivIVA-like N-terminal domains per hexamer (Rismondo *et al.*, 2016, Cleverley *et al.*, 2016). PBP A1 binds to a conserved cavity in the N-terminal domain of GpsB, which is present twice in the dimeric N-terminal domain (Rismondo *et al.*, 2016). Thus, up to six PBP A1 molecules could interact with the GpsB hexamer. Most likely, GpsB mediates spatial clustering of PBP A1 or brings together PBP A1 with other divisome components (Egan *et al.*, 2017).

During further investigations of the Δ*gpsB* phenotype, we noticed that the Δ*gpsB* mutant revealed an increased resistance against lysozyme. Given the increased penicillin susceptibility of the Δ*gpsB* mutant (Rismondo *et al.*, 2016), this was a counter-intuitive observation and thus we studied this phenomenon in more detail. We demonstrate here that deletion of *pbpA1* suppressed the lysozyme resistant phenotype of the Δ*gpsB* mutant, providing further support for control of PBP A1 through GpsB. Analysis of lysozyme resistance in mutant strains lacking or depleted for all five high molecular weight penicillin binding proteins (HMW PBPs) revealed that depletion of PBP B1 specifically increased lysozyme resistance, but in a PBP A1-independent manner. Combinatorial gene deletions showed that the increased lysozyme resistance of the Δ*gpsB* mutant is OatA-independent but PgdA-dependent. Increased peptidoglycan deacetylation was verified by muropeptide analysis, indicating that GpsB is a critical determinant for control of the peptidoglycan deacetylase PgdA in *L. monocytogenes*. Finally, PgdA interacted with PBP A1 in bacterial two hybrid experiments and truncations revealed that both proteins bind each other via their single transmembrane domains. This shows that GpsB exerts its effect on PgdA through PBP A1 and we propose that PgdA is associated with PBP A1 in *L. monocytogenes*.

RESULTS

GpsB affects lysozyme resistance

We have shown earlier that lack of *gpsB* leads to defects in peptidoglycan biosynthesis and this is reflected by a reduced resistance of *L. monocytogenes* against penicillin (Rismondo *et al.*, 2016). We assumed that a weakened peptidoglycan sacculus should also lead to an increased susceptibility against enzymes degrading the cell wall, such as the muramidase lysozyme, which cleaves the β-1,4-linkages between N-acetylmuramic acid and N-acetylglucosamine. *L. monocytogenes* is particularly lysozyme resistant and this is explained by N-deacetylation and O-acetylation of N-acetylglucosamine and N-acetylmuramic acid, respectively, in their peptidoglycan (Boneca *et al.*, 2007, Aubry *et al.*, 2011, Rae *et al.*, 2011).

We have tested the susceptibility of *gpsB* mutant strains against lysozyme in quantitative lysis assays. This revealed that only 3.6±0.8% of the initially applied wild type cells survived exposure to lysozyme for 120 min. In contrast, 20.5±4.5% of the Δ*gpsB* mutant cells endured this treatment and this was in contrast to our initial assumption (Fig. 1A). Concomitantly, 4.4±0% of the initially applied IPTG-inducible *gpsB* mutant LMS56 (I*gpsB* - this syntax is used throughout the manuscript to denote conditional strains containing a deletion of the chromosomal gene and an IPTG-inducible gene copy at an ectopic site) cells did not lyse after 120 min, when the cells were pre-grown in the presence of IPTG. However, 10.6±1.1% of the inoculum had not undergone lysis in the absence of the inducer (Fig. 1A). Based on these data, half-life periods were calculated to describe lytic decay more precisely. Half-life of wild type cells in the presence of 2.5 µg/ml lysozyme was 25.7 min and this value was nearly doubled in the Δ*gpsB* mutant ($T_{1/2}$=49.7 min). Half-life of the inducible *gpsB* mutant (LMS56) was similar to wild type in the presence of IPTG ($T_{1/2}$=24.7 min) and increased to 36.5 min, when no IPTG was added. These

results collectively indicate that GpsB is implicated in control of *L. monocytogenes* lysozyme susceptibility, and that its absence leads to increased lysozyme resistance.

Lysozyme resistance of Δ*gpsB* cells depends on PBP A1

GpsB is inherently linked to penicillin binding protein A1 (PBP A1) and several aspects of the complex Δ*gpsB* phenotype are at least partially cured by deletion of *pbpA1* (Rismondo *et al.*, 2016). In order to test, whether *pbpA1* deletion also suppressed the increased lysozyme resistance of the Δ*gpsB* mutant, lysis assays were repeated with strains lacking *gpsB* (strain LMJR19), *pbpA1* (LMS57) or both (LMJR38). Only 5.4±1.0% of the wild type inoculum resisted the lysozyme exposure ($T_{1/2}$=27.7 min), whereas 39.7±2.5% of the Δ*gpsB* cells did not lyse in this experiment ($T_{1/2}$=86.6 min, Fig. 1B). The Δ*pbpA1* cells were just slightly but not significantly more resistant against lysozyme than the wild type (10.6±4.6% surviving cells, $T_{1/2}$=34.7 min). Experiments with an inducible *pbpA1* mutant (I*pbpA1*, strain LMJR21) did also not resolve differences in lysozyme resistance in the presence or absence of IPTG (data not shown). However, only 9.1±0.4% cells of the Δ*gpsB* Δ*pbpA1* double mutant overcame the lysozyme exposure ($T_{1/2}$=31.5 min), demonstrating that the increased lysozyme resistance of the Δ*gpsB* mutant is suppressed in the Δ*gpsB* Δ*pbpA1* double mutant. The shape of its lysis curve indicates that this strain is even more sensitive to lysozyme than the wild type at early time points (Fig. 1B). The Δ*gpsB* mutant has a growth defect compared to wild type at 37°C but grows with similar rate as the lysozyme-sensitive Δ*gpsB* Δ*pbpA1* mutant (Fig. 1C). Moreover, autolysis of the Δ*gpsB* mutant in the absence of lysozyme is negligible (Fig. S1), ruling out the possibility that differences in growth or autolysis rates account for the increased lysozyme resistance in the Δ*gpsB* mutant. These results indicate that GpsB contributes to lysozyme resistance of *L. monocytogenes* in a process that involves PBP A1.

Next to PBP A1, *L. monocytogenes* contains PBP A2, a second bi-functional penicillin binding protein with glycosyltransferase and transpeptidase activity. Moreover, three monofunctional transpeptidases are present: PBP B1, required for rod-shape, PBP B2, a division-specific transpeptidase and PBP B3, so far only linked to penicillin resistance (Korsak *et al.*, 2010, Guinane *et al.*, 2006, Rismondo *et al.*, 2015). The effect of the four remaining HMW PBPs (PBP A2 and PBP B1-3) on lysozyme resistance of the Δ*gpsB* mutant could only partially be tested since the Δ*gpsB* mutant did not grow after depletion of PBP A2 (Rismondo *et al.*, 2016) or after depletion of PBP B1 (see below) and since depletion of PBP B2 was lethal even in wild type bacteria (Rismondo *et al.*, 2015). A Δ*gpsB* Δ*pbpB3* mutant was viable though, but inactivation of *pbpB3* did not affect lysozyme resistance of Δ*gpsB* mutant cells (Fig. S2). Hence, the effect of PBP A1 on lysozyme resistance of the Δ*gpsB* mutant seems to be specific for PBP A1 as far as this could be tested.

A structural role for PBP A1 in control of lysozyme resistance

PBP A1 is one of the two bi-functional penicillin binding proteins in *L. monocytogenes* mediating elongation of peptidoglycan strands through glycosyltransfer reactions and the subsequent crosslinking of stem peptides through transpeptidation (Rismondo *et al.*, 2015, Korsak *et al.*, 2010, Sauvage *et al.*, 2008). Besides these two enzymatic functions, PBP A1 also serves as a scaffold for interaction with components of the divisome and elangosome complexes such as FtsL and MreB, respectively (Claessen *et al.*, 2008, Kawai *et al.*, 2009). Suppression of the enhanced lysozyme resistance of the Δ*gpsB* mutant through *pbpA1* deletion may thus be explained by loss of enzymatic PBP A1 activity or by loss of PBP A1 as an interaction partner. The two enzymatic activities of *Escherichia coli* PBP1A, which corresponds to PBP A1 of *L. monocytogenes*, can be inactivated by mutation of glutamate 94 in its glycosyltransferase domain,

because cross-linking of the peptide stems of the growing glycan strands requires ongoing glycosyltransferase reactions (Born *et al.*, 2006). The analogous residue in *L. monocytogenes* PBP A1 is glutamate 116. Thus, an E116A mutation (Fig. 2A) was introduced into an ectopic IPTG-inducible *pbpA1-flag* allele and combined with a chromosomal *pbpA1* deletion in strain LMJR51 (I*pbpA1E116A-flag*). This allele was inactive, since it could not complement the morphological defects associated with a *pbpA1* deletion (Rismondo *et al.*, 2015) as determined by phase contrast microscopy (Fig. 2B), even though PBP A1 E116A-Flag was similarly expressed as PBP A1-Flag (data not shown). In order to test whether enzymatic or structural functions of PBP A1 contribute to lysozyme resistance, the effect of the *pbpA1E116A* mutation on lysozyme resistance of the Δ*gpsB* mutant was analyzed. For this purpose, lysozyme resistance was measured in strains LMJR60 (Δ*gpsB* I*pbpA-flag*) and LMJR57 (Δ*gpsB* I*pbpA1E116A-flag*) in the presence of IPTG. While the wild type ($T_{1/2}$=28.9 min) and the Δ*gpsB* Δ*pbpA1* double mutant ($T_{1/2}$=27.7 min) showed the described lysozyme-sensitive lysis kinetics, strain LMJR60 (Δ*gpsB* I*pbpA-flag*, $T_{1/2}$=46.2 min) behaved like the Δ*gpsB* mutant ($T_{1/2}$=46.2 min) under this condition (Fig. 2C). Interestingly, strain LMJR57 (Δ*gpsB* I*pbpA1E116A-flag*) was as resistant to lysozyme as the Δ*gpsB* strain ($T_{1/2}$=49.5 min, Fig. 2C), showing that the *pbpA1E116A* mutation, although enzymatically inactivating PBP A1, does not suppress the increased lysozyme resistance associated with loss of *gpsB*. These results indicate that PBP A1 rather serves a structural than an enzymatic function in the context of lysozyme resistance.

Effect of other high molecular weight PBPs on lysozyme resistance

Despite the fact that PBP A1 appears to be the major GpsB target (Rismondo *et al.*, 2016), GpsB also interacted with the PBP A2, B1, B2 and B3 in bacterial two hybrid experiments (unpublished results). In order to test the contribution of the remaining four of the five high molecular weight

204 penicillin binding proteins to lysozyme resistance of *L. monocytogenes*, mutant strains lacking or
205 conditionally expressing their corresponding genes (Rismondo *et al.*, 2015) were analyzed in
206 lysis assays. This confirmed that only 1.4±1.4% of the wild type cell inoculum overcame the
207 lysozyme treatment ($T_{1/2}$=19.8 min) and that the mutant lacking the bi-functional penicillin
208 binding protein PBP A1 was somewhat (but not significantly) more resistant (6.7±1.4%
209 survivors, $T_{1/2}$=31.5 min). Likewise, deletion of the second bi-functional PBP, PBP A2, caused
210 slightly increased lysozyme resistance (8.2±1.5% survivors, $T_{1/2}$=33 min, Fig. 3A). Lysozyme
211 resistance was only modestly affected in cells depleted for PBP B2 (3.1±0.8% survivors,
212 $T_{1/2}$=25.7 min) and not affected at all in cells lacking PBP B3 (1.4±1.4% survivors, $T_{1/2}$=18.7
213 min, Fig. 3A). Strikingly, depletion of PBP B1 in LMJR27 cells caused severely increased levels
214 of lysozyme resistance. This even exceeded the Δ*gpsB* effect, as 40.7±1.5% of the LMJR27
215 inoculum was not lysed at the end of the lysozyme exposure ($T_{1/2}$=86.6 min), when the cells were
216 pre-grown in the absence of IPTG, as compared to 21.1±4.1% non-lysed Δ*gpsB* cells ($T_{1/2}$=53.3
217 min, Fig. 3A). However, lysozyme resistance of LMJR27 cells was shifted back to the normal
218 wild type level (0.9±0.8% survivors, $T_{1/2}$=19.3 min) in the presence of IPTG (Fig. 3A).
219 The contribution of PBP A1 to the PBP B1 effect was tested in a separate experiment. For this
220 purpose, *pbpA1* was removed in the PBP B1 depletion strain, resulting in strain LMJR81
221 (Δ*pbpA1* I*pbpB1*). 48±3.6% of the PBP B1-depleted LMJR81 (Δ*pbpA1* I*pbpB1*) inoculum
222 endured the lysozyme treatment ($T_{1/2}$=99 min), compared to 52.3±5.4% of the PBP B1-depleted
223 LMJR27 (I*pbpB1*) cells (Fig. 3B). This shows that PBP A1 only contributes to a minor extent to
224 the massive increase of lysozyme resistance upon PBP B1 depletion, which in turn suggests that
225 the effects of GpsB and PBP B1 on lysozyme resistance are independent from each other. In
226 order to test whether both effects add up in a *gpsB pbpB1* double mutant, we constructed strain

LMJR76 (Δ*gpsB* I*pbpB1*), which lacks *gpsB* and requires IPTG for expression of the *pbpB1* gene. However, this strain cannot grow in the absence of IPTG (Fig. S3).

Lysozyme resistance of Δ*gpsB* cells is OatA-independent

O-acetylation of N-acetylmuramic acid by the O-acetyltransferase OatA is one mechanism employed by *L. monocytogenes* to confer lysozyme resistance to its peptidoglycan sacculus (Rae *et al.*, 2011, Aubry *et al.*, 2011). Thus, the *oatA* gene was deleted from the genome of the Δ*gpsB* mutant and growth of the resulting Δ*gpsB* Δ*oatA* strain (LMS166) was compared to both single mutants. This revealed the absence of any growth anomalies for the Δ*oatA* mutant and showed that the Δ*gpsB* Δ*oatA* double mutant grows like the Δ*gpsB* single mutant strain (Fig. 4A). As reported previously (Rae *et al.*, 2011, Aubry *et al.*, 2011), deletion of *oatA* reduced lysozyme resistance also in our hands ($T_{1/2}$=26.7 min compared to $T_{1/2}$=34.7 min for wild type in this experiment, Fig. 4B). However, deletion of *oatA* was not dominant over the Δ*gpsB* allele with respect to its effect on lysozyme resistance: While 44.1±2.7% of the Δ*gpsB* cells survived the lysozyme treatment ($T_{1/2}$=99 min), 26.8±5.7% of the Δ*gpsB* Δ*oatA* double mutant cells were still not lysed after the end of the 120 min interval ($T_{1/2}$=57.8 min, Fig. 4B). As a control, disintegration of both, the Δ*oatA* single and the Δ*gpsB* Δ*oatA* double mutant was tested in the absence of lysozyme and no effect was observed (Fig. S4A). This clearly shows that O-acetylation by OatA is only of minor importance for the increased lysozyme resistance of the Δ*gpsB* mutant.

Lysozyme resistance of Δ*gpsB* cells depends on PgdA

The second mechanism by which *L. monocytogenes* renders its peptidoglycan resistance to degradation by lysozyme is N-deacetylation of N-acetylglucosamine residues through PgdA

(Boneca *et al.*, 2007). To assess the contribution of PgdA to the Δ*gpsB* lysozyme effect, we tried to delete the *pgdA* gene in the Δ*gpsB* background. However, this was not successful, despite repeated attempts, suggesting synthetic lethality of this allelic combination. In contrast, deletion of *pgdA* was possible in strain LMS56 (I*gpsB*), as long as the procedure was carried out in the presence of IPTG. As expected, growth of the resulting Δ*pgdA* I*gpsB* strain (LMS170) was clearly IPTG-dependent, whereas the Δ*pgdA* single mutant grew as fast as the wild type (Fig. 4C). This confirmed that lack of PgdA is not tolerated in the absence of GpsB and we assume that protection against the listerial autolysins through PgdA-dependent N-deacetylation may become critical under conditions of distorted cell wall biosynthesis as they occur in the absence of GpsB.

Deletion of *pgdA* massively reduced resistance of *L. monocytogenes* against lysozyme ($T_{1/2}$=8.0 min) compared to wild type ($T_{1/2}$=26.7 min, Fig. 4D). Most Δ*pgdA* cells were already lysed within the first 30 minutes of lysozyme exposure (4.1±1.3% non-lysed cells after 30 min). The same lysis curve was observed for the Δ*pgdA* I*gpsB* strain LMS170, when grown with IPTG (4.2±0.6% non-lysed cells after 30 min, $T_{1/2}$=7.8 min). Depletion of GpsB in this strain counteracted this effect only slightly (19.9±3.9% intact cells after 30 min, $T_{1/2}$=13.9 min), whereas 67.3±4% of the initially applied inoculum was still not disintegrated after 30 minutes in the Δ*gpsB* mutant strain LMJR19 ($T_{1/2}$=69.3 min, Fig. 4D). In contrast, *pgdA* and *gpsB* did not substantially affect intrinsic autolysis in the absence of lysozyme (Fig. S4B). These results unequivocally demonstrate that the deletion of *pgdA* is dominant over the Δ*gpsB* deletion with regard to its effect on lysozyme resistance and show that the increased lysozyme resistance of the Δ*gpsB* mutant depends on PgdA. It thus seems likely that PgdA becomes overactive upon deletion of *gpsB*.

Deletion of *oatA* or *pgdA* is synthetic lethal with depletion of PBP B1

Contrary to deletion of *gpsB*, depletion of PBP B1 is known to cause reduced N-deacetylation in *L. monocytogenes* (Rismondo *et al.*, 2015), suggesting that the increased lysozyme resistance in PBP B1-depleted cells is caused by processes other than PgdA-dependent peptidoglycan N-deacetylation. In order to test this hypothesis, the *pgdA* and *oatA* genes were removed from the genomes of the IPTG-inducible *pbpB1* mutant, resulting in strains LMS171 (Δ*pgdA* I*pbpB1*) and LMS172 (Δ*oatA* I*pbpB1*). Both mutants as well as strain LMJR27 (I*pbpB1*) were pre-grown in BHI broth with IPTG over night and then used to inoculate cultures containing or not containing 1 mM IPTG the next morning. As reported recently, depletion of PBP B1 in strain LMJR27 (I*pbpB1*) led to a considerable deceleration, but not to a complete cessation, of growth (Rismondo *et al.*, 2015), most likely explained by leakiness of the un-induced P_{help} promoter (Monk *et al.*, 2008). In contrast, depletion of PBP B1 in strains LMS171 (Δ*pgdA* I*pbpB1*) and LMS172 (Δ*oatA* I*pbpB1*) resulted in a complete growth arrest, as these cells underwent only 1-2 doublings and then stopped to proliferate, whereas Δ*pgdA* and Δ*oatA* single mutants grew as fast as the wild type strain (Fig. S5). Apparently, absence of both peptidoglycan-modifying systems becomes lethal in the absence of PBP B1. It is tempting to speculate that PgdA-dependent N-deacetylation and OatA-dependent O-acetylation also protect the listerial cell wall against hydrolysis by its own autolysins, especially endopeptidases such as p60 (Vollmer *et al.*, 2008), when PBP B1-dependent transpeptidation is disturbed.

Increased N-deacetylation in Δ*gpsB* peptidoglycan

If PgdA is overactive in cells lacking *gpsB*, then the peptidoglycan of the Δ*gpsB* mutant should reveal increased N-deacetylation rates compared to wild type. In order to test this hypothesis, cell walls were isolated from strains EGD-e (wt), LMJR19 (Δ*gpsB*) and LMS56 (I*gpsB*) grown in the

298 presence of IPTG. Peptidoglycan strands were hydrolyzed using the muramidase cellosyl and the
299 resulting muropeptides were separated by high pressure liquid chromatography. The nature of the
300 main muropeptide peaks is known from previously published ESI-MS/MS data (Rismondo *et al.*,
301 2015). This revealed two remarkable alterations in the muropeptide pattern of the Δ*gpsB* mutant
302 that are corrected back to the wild type situation in the muropeptide profile obtained with the
303 complemented strain LMS56 (Fig. 5A-C). First, the Δ*gpsB* mutant showed an increase in the
304 deacetylated muropeptide species Tri[deAc] and TetraTri[deAc]$_2$, and second, the fraction of the
305 double acetylated muropeptide TetraTri is reduced in the absence of *gpsB*. These results are
306 consistent with the idea of hyperactive N-deacetylation in the Δ*gpsB* mutant. The effect of *pbpA1*
307 on peptidoglycan N-deacetylation in the Δ*gpsB* mutant was tested separately. This showed that
308 the increased fractions of the deacetylated Tri[deAc] (peak no. 2 in Fig. S6) and TetraTri[deAc]$_2$
309 (peak no. 6) muropeptides observed in the Δ*gpsB* mutant were corrected back to nearly wild type
310 levels in the Δ*gpsB* Δ*pbpA1* strain. Likewise, the reduced amount of the double acetylated
311 TetraTri muropeptide (peak no. 3) seen in the Δ*gpsB* mutant was corrected to a wild type-like
312 level in the Δ*gpsB* Δ*pbpA1* double mutant. The combined fraction of fully acetylated
313 muropeptides was calculated as 57.7±0.6% in the wild type, dropped down to 52.8±1.4% in the
314 Δ*gpsB* strain and was shifted back to 59.3±0.6% in Δ*gpsB* Δ*pbpA1* mutant. In conclusion, GpsB
315 affects peptidoglycan N-deacetylation in a PBP A1-dependent manner.
316
317 **PgdA forms a complex with PBP A1**
318 GpsB has been described as an interaction partner of PBP A1 in *L. monocytogenes* and *B. subtilis*
319 (Rismondo *et al.*, 2016, Claessen *et al.*, 2008), and based on the genetic data explained above we
320 speculated that PBP A1 could interact with PgdA. This idea seems reasonable since deacetylation
321 likely occurs right after glycosyltransfer and transpeptidation of peptidoglycan chains by PBP A1

at the cell surface. We tested a possible interaction between both proteins using the bacterial two hybrid system. GpsB strongly interacted with itself in this assay, as described earlier (Rismondo *et al.*, 2016), and bound the T18- and T25-fragments fused to the cytosolic N-terminus of PBP A1 in all tested permutations. These PBP A1 fusions also showed self-interactions (Fig. 6A). Dimerization of PBP A1 would be in good agreement with earlier results obtained by Bertsche *et al.* (Bertsche *et al.*, 2005), demonstrating dimerization of the bi-functional glycosyltransferase/transpeptidase PBP1B of *E. coli*. The two PgdA fusion proteins self-interacted, but more interestingly, they both interacted with PBP A1 (Fig. 6A). In contrast, an interaction between PgdA and GpsB was not detected (Fig. 6A). It is tempting to speculate that all three proteins participate in a tripartite GpsB-PBP A1-PgdA complex *in vivo*, in which PgdA is linked to GpsB via PBP A1 (Fig. 6B).

Both, PgdA and PBP A1 are single-spanning transmembrane proteins with a short cytosolic N-terminus and large C-terminal portions presented outside the cell (Renier *et al.*, 2012). The extracellular part of PBP A1 is composed of a glycosyltransferase (GT, amino acids 92-288) fused to a transpeptidase domain (TP, 324-641) at the C-terminus. The extracellular part of PgdA folds into three distinct domains: an N-terminal domain (N, 29-158), a middle domain (M, 159-266) and a C-terminal catalytic domain (C, 267-466) (Blair *et al.*, 2005). In order to determine, which domain establishes the contact between PBP A1 and PgdA, the transpeptidase (ΔTP) or the transpeptidase and the glycosyltransferase domains (ΔGT-TP) were deleted from the T25-PBP A1 fusion and tested in the bacterial two hybrid assay for their interaction with full length T25-PgdA and truncations thereof, which lack the C-terminal (ΔC), the C-terminal and the middle (ΔMC) or the C-terminal, the middle and the N-terminal (ΔNMC) domain. This approach showed that the 91 amino acids long PBP A1ΔGT-TP fragment, which basically consists of the transmembrane domain (amino acids 33-55) plus short N- and C-terminal extensions, still

interacted with full length PgdA (Fig. 6C). Likewise, the N-terminal PgdAΔNMC fragment (1-28) comprising the transmembrane domain (8-26) and a short N-terminal extension was still capable to bind to PBP A1. Strikingly, the PBP A1ΔGT-TP peptide still interacted with PgdAΔNMC (Fig. 6C) and this strongly suggested that both proteins bind each other using their transmembrane helices (Fig. 6D).

Importance of the PBP A1-PgdA interaction for peptidoglycan N-deacetylation

For identification of those amino acids in the transmembrane helix of PgdA that contribute to PBP A1 binding, an alanine mutagenesis screen was performed. The transmembrane domain of PgdA spans residues 8-26 according to an *in silico* prediction using the TMpred algorithm (Hofmann & Stoffel, 1993). We systematically exchanged all amino acids in this region into alanine residues in the PgdAΔNMC T25-fusion and tested the effect of these mutations on the interaction with full-length PBP A1 and full-length PgdA. This revealed that the amino acid exchanges R7A, I15A and V19A prevented PBP A1 and PgdA binding, whereas the amino acid exchanges W5A and L8A only affected PgdA dimerization (Fig. 7A). According to the positive inside rule, positively charged amino acids such as R7 are often found directly at the cytosolic end of transmembrane fragments (Heijne, 1986). They favor membrane insertion of hydrophobic helices as they interact with surrounding negatively charged phospholipid head groups (Lerch-Bader *et al.*, 2008). Presumably, the R7A mutation affects membrane insertion of PgdA. More importantly, however, residues I15 and V19 are separated by exactly one turn in the helix and oriented towards the same face. In contrast, residues W5 and L8 are spatially separated from this motif and part of the cytosolic N-terminus (Fig. 7B).

In order to measure the contribution of the PgdA-PBP A1 interaction to PgdA function and, thus, to lysozyme resistance, all five *pgdA* mutations were introduced into the chromosomal *pgdA* gene

and the resulting strains were analyzed in quantitative lysis assays (Fig. 7C). This demonstrated that all but one *pgdA* mutant (V19A) indeed displayed reduced resistance against lysozyme. For a more quantitative comparison, half-life periods were calculated based on averaged lysis curves (n=3). This procedure showed that half-life of wild type bacteria in the presence of lysozyme is roughly half an hour ($T_{1/2}$=26.7 min) and lysozyme-induced lysis is accelerated almost four-fold in the Δ*pgdA* strain ($T_{1/2}$=7.2 min). Half-life of the V19A mutant ($T_{1/2}$=27.7 min) was comparable to wild type, but lysozyme resistance decreased in the I15A ($T_{1/2}$=23.1) and the L8A ($T_{1/2}$=21.6 min) mutants. Stronger reductions in lysozyme resistance were observed with the R7A ($T_{1/2}$=15.8 min) and W5A ($T_{1/2}$ = 16.5 min) strains. Taken together, we conclude that the interaction of PgdA with PBP A1 contributes to full PgdA activity.

DISCUSSION

GpsB is a DivIVA-like cell division protein in firmicute bacteria and has been linked to control of peptidoglycan biosynthesis in *Bacillus subtilis*, *Streptococcus pneumoniae* and *Listeria monocytogenes* (Claessen *et al.*, 2008, Land *et al.*, 2013, Rismondo *et al.*, 2016, Fleurie *et al.*, 2014). GpsB controls cell wall synthesis through an interaction with PBP A1, which is one of the two bi-functional high molecular weight penicillin binding proteins in *L. monocytogenes*. These proteins catalyze insertion of peptidoglycan precursors into growing PG strands by glycosyltransfer reactions and their subsequent crosslinking by transpeptidation (Rismondo *et al.*, 2015, Korsak *et al.*, 2010, Sauvage *et al.*, 2008). PBP A1 contributes to peptidoglycan biosynthesis at the cross wall during cell division and at the cylindrical parts of the cell to ensure cell elongation (Rismondo *et al.*, 2016). GpsB binding is required for PBP A1 function and GpsB seems to control spatial clustering of PBP A1 or its association with other proteins engaged in cell wall biosynthesis and cell division (Rismondo *et al.*, 2016, Egan *et al.*, 2017).

Besides its importance for cell wall biosynthesis, GpsB contributes to cell wall modification, as we demonstrate here. Absence of GpsB had a pronounced effect on lysozyme resistance, which could be caused by overactive PgdA or OatA enzymes, but genetic experiments made clear that GpsB must affect activity of PgdA. In good agreement with this result is the observation that N-deacetylated muropeptides accumulated in the Δ*gpsB* mutant strain, leading to the conclusion that PgdA activity is increased in the absence of GpsB. This hyperactivity of PgdA in the Δ*gpsB* mutant is suppressed in the absence of PBP A1, indicating that PBP A1 provides a link between GpsB and PgdA-dependent peptidoglycan N-deacetylation and that PBP A1 enhances the activity of PgdA. PBP A1 and PgdA are both integral transmembrane proteins with a single transmembrane helix, which are preceded by short cytosolic tails, at their N-termini (Vollmer &

406 Tomasz, 2000, Korsak *et al.*, 2010). The cytosolic tail of PBP A1 is 32 amino acids long and
407 GpsB interacts with PBP A1 via this region (Rismondo *et al.*, 2016). In contrast, only seven N-
408 terminal amino acids precede the transmembrane helix of PgdA (residues 8-26), so an interaction
409 of GpsB with PgdA via this region seemed unlikely. In better agreement with our genetic data
410 would be the assumption that PgdA exists in a complex with PBP A1. In such a case, deletion of
411 *gpsB* would relieve PBP A1 from control through GpsB and thus PgdA would become as
412 deregulated as PBP A1. Formation of a complex between PBP A1 and PgdA is supported by
413 bacterial two hybrid data, which even showed that both proteins interact via their transmembrane
414 domains. Lysozyme resistance is diminished in strains with mutations in the PBP A1 interaction
415 site of PgdA. Thus, the interaction between PBP A1 and PgdA contributes to normal PgdA
416 activity levels. Deacetylation of peptidoglycan is the enzymatic step in peptidoglycan maturation
417 that directly follows transglycosylation and transpeptidation through penicillin binding proteins.
418 Physical interactions between consecutive enzymes in a pathway can help to increase overall
419 efficiency of metabolic pathways, as it is observed with glycolytic enzymes in different bacteria
420 (Commichau *et al.*, 2009, Dutow *et al.*, 2010). A tight coupling between PBP A1 and PgdA could
421 thus explain why half of all GlcNAc residues are N-deacetylated in *L. monocytogenes* (Boneca *et*
422 *al.*, 2007). Conceivably, PBP A1 recruits PgdA to sites of active peptidoglycan biosynthesis,
423 where PgdA could be more active than elsewhere.
424 Inactivation of *clpC* (encoding an ATPase subunit of the proteasome), of *murZ* (encoding an
425 UDP-GlcNAc 1-carboxyvinyltransferase) and of genes encoding other UDP-GlcNAc consuming
426 enzymes (GtcA, Lmo2550) also suppress the phenotype of the Δ*gpsB* mutant, at least its growth
427 defect at higher temperature (Rismondo *et al.*, 2017). It has been assumed that these suppressor
428 mutations compensate the effects of PBP A1 inefficiency by redirection of additional precursor
429 molecules into the peptidoglycan biosynthetic pathway (Rismondo *et al.*, 2017). We measured

the effect of two such suppressor mutations (*clpCR254S* and *murZ*$^{1\text{-}253}$) on lysozyme resistance of the Δ*gpsB* mutant and found that resistance against lysozyme is corrected back to wild type level in these strains (Fig. S7). It has been shown that MurA, which is the primary UDP-GlcNAc 1-carboxyvinyltransferase of *L. monocytogenes* and catalyzes the first committed step of peptidoglycan biosynthesis, is approximately ten-fold overproduced in these suppressor strains, leading to redirection of precursors into cell wall biosynthesis (Rismondo *et al.*, 2017). In contrast, *pbpA1* inactivation does not affect the MurA protein level at all (Rismondo *et al.*, 2017). We hence assume that suppression of the Δ*gpsB* mutant´s increased lysozyme resistance can occur by two mechanisms: (i) By deletion of *pbpA1*, neutralizing uncontrolled and deregulated peptidoglycan biosynthesis through PBP A1, and (ii) by activation of precursor influx into peptidoglycan synthesis. Both mechanisms would readjust the incorporation rate of cell wall precursors into the growing peptidoglycan network to the normal N-deacetylation capacity provided by PgdA. Apparently, the precise coordination of peptidoglycan production and its N-deacetylation determines resistance against lysozyme in the end. Any mutation that would increase the rate of peptidoglycan biosynthesis would thus affect the equilibrium between synthesis and N-deacetylation and should thus lessen the fraction of N-deacetylated muropeptides in the cell wall. On the other hand, any mutation that reduces peptidoglycan production should lead to increased N-deacetylation rates and thus to higher resistance against lysozyme.

Interestingly, depletion of PBP B1, which had been implicated in maintenance of rod shape and cell wall integrity, caused an even stronger increase of lysozyme resistance than in the Δ*gpsB* mutant. This is remarkable for two reasons: (i) Previous work revealed reduced PgdA activity in PBP B1-depleted cells (Rismondo *et al.*, 2015), and (ii) PBP B1-depleted cells show a high rate of spontaneous autolysis in the absence of cell wall degrading agents (Rismondo *et al.*, 2015), a phenotype that should promote overall bacteriolysis, in particular in the presence of lysozyme.

454 The contribution of the two known peptidoglycan modifying enzymes affecting lysozyme
455 resistance could not be studied, since deletion of *oatA* and *pgdA* turned out to be synthetic lethal
456 with depletion of PBP B1. While it remains to be seen if other structural changes determine the
457 increased lysozyme resistance in PBP B1-depleted cells, all together our data show that
458 peptidoglycan deacetylation by PgdA is affected by the major peptidoglycan synthesis enzymes,
459 and this is due to direct protein-protein interactions.
460

MATERIALS AND METHODS

Bacterial strains and growth conditions

Table 1 lists all strains used in this study. Strains of *L. monocytogenes* were generally cultivated in BHI broth or on BHI agar plates at 37°C if not stated otherwise. Where required, antibiotics and supplements were added at the following concentrations: erythromycin (5 µg/ml), kanamycin (50 µg/ml), X-Gal (100 µg/ml) and IPTG (1 mM). *Escherichia coli* TOP10 was used as standard cloning host (Sambrook *et al.*, 1989).

General methods, manipulation of DNA and oligonucleotide primers

Transformation of *E. coli*, isolation of plasmid DNA and chromosomal DNA was performed using standard methods (Sambrook *et al.*, 1989). Transformation of electro-competent *L. monocytogenes* was carried out as described by others (Monk *et al.*, 2008). Restriction and ligation of DNA was performed as described by the manufacturer´s instructions. All primer sequences are listed in table 2.

Construction of plasmids and strains

All plasmids used in this study are listed in table 1. Plasmid pSH401 was constructed for removal of *pgdA*. For this purpose, regions lying up- and downstream of *pgdA* were amplified with the primer pairs SHW553/SHW555 and SHW556/554, respectively. Both fragment were cut with PstI and ligated together. The desired fusion product was amplified from the ligation mixture in a second PCR using the oligonucleotides SHW553/SHW554 and cloned into pMAD using BglII/SalI. For deletion of *oatA*, plasmid pSH402 was constructed. The *oatA* up- and downstream regions were amplified with SHW561/SHW564, and SHW563/562, respectively, and cut using

SalI. Both fragments were fused together by ligation. The desired fusion product was amplified from the ligation mixture in a second PCR using the primer pair SHW561/SHW562 and cloned into pMAD using BamHI/NcoI.

Plasmid pSW1 was constructed as the first step towards the deletion of the *pgdA* N-terminus. This plasmid was obtained after amplification of a *pgdA´* fragment from EGD-e chromosomal DNA with primers SW1/SW2 and cloning of the obtained PCR product into pMAD using BamHI/NcoI. The first 460 nucleotides of *pgdA* were deleted from plasmid pSW1 in a PCR using the primers SW3/SW4 and this procedure yielded plasmid pSW2. Point mutations were introduced into the N-terminus of *pgdA* of plasmid pSW1 by quikchange mutagenesis (Zheng *et al.*, 2004) using the oligonucleotides SHW693/SW9 (W5A), SHW697/SW10 (R7A), SHW699/SW11 (L8A), SHW711/SHW712 (I15A) and SHW717/SHW718 (V19A).

Plasmid pJR34 was constructed for inducible expression of PBPA1E116A-Flag. This plasmid was obtained by quikchange mutagenesis with primers JR111/JR112 and plasmid pJR33 as the template.

pMAD plasmids were introduced into the respective recipient strains by electroporation and erythromycin resistant transformants were selected at 30°C. Genes were deleted/inserted using a plasmid integration/excision strategy described by others (Arnaud *et al.*, 2004). All insertions and deletions were verified by PCR.

For bacterial two hybrid analysis, the *pgdA* gene was amplified using the primer pair SHW666/SHW667 and cloned into the XbaI/KpnI sites of pKT25, yielding pSH432. The XbaI/KpnI *pgdA* fragment of pSH432 was then subcloned into pUT18C, resulting in pJR141. In order to generate plasmid pJR140, the XbaI/KpnI *pbpA1* fragment of plasmid pSH234 was subcloned into pUT18C. The PBP A1 transpeptidase domain was deleted from plasmid pSH234 by PCR using the primer pair SHW672/SHW673, yielding plasmid pSH436. Likewise, the

glycosyltransferase and the transpeptidase domains were deleted from pSH234 using the primer pair SHW672/SHW674, which yielded plasmid pSH437. A fragment encoding the C-terminal PgdA domain was deleted from plasmid pJR141 by PCR using the primers SHW675/SHW676, yielding pSH438. The C-terminal and the middle domain encoding regions were deleted from pJR140 using the primers SHW675/SHW677, resulting in pSH439. Finally, a fragment encoding the C-terminal, the middle and the N-terminal domains was deleted from plasmid pJR140 in a PCR using the primer pair SHW675/SHW678 and this yielded plasmid pSH440.

Quikchange mutagenesis was used to introduce the following amino acid exchanges into the *pgdA* fragment expressed from plasmid pSH440: W5A (SHW693/SHW694), I6A (SHW695/SHW696), R7A (SHW697/SHW698), L8A (SHW699/SHW700), S9A (SHW701/SHW702), L10A (SHW703/SHW704), V11A (SHW705/SHW706), I13A (SHW707/SHW708), I15A (SHW711/SHW712), I16A (SHW713/SHW714), V18A (SHW715/SHW716), V19A (SHW717/SHW718), F20A (SHW719/SHW720), I21A (SHW721/SHW722), V23A (SHW723/SHW724), I24A (SHW725/SHW726), F26A (SHW727/SHW728).

Lysis assay

L. monocytogenes strains were grown in BHI broth (containing 1 mM IPTG where required) at 37°C until an optical density of around OD_{600}=0.8 was reached. Cells were collected by centrifugation (6000 x *g*, 5 min, 4°C) and resuspended in 50 mM Tris/HCl pH8.0 to an optical density of OD_{600}=0.6. Lysozyme (2.5 µg/ml final concentration) was added where indicated and the cells were shaken at 37°C. Lysis was followed by measuring the decrease in optical density (λ=600 nm) every 15 min in a spectrophotometer. Significance levels were calculated using the unpaired *t*-test.

Bacterial two hybrid analysis

Interactions of PgdA with PBP A1 and GpsB were studied by the bacterial two hybrid system (Karimova *et al.*, 1998). Plasmids encoding PgdA, PBP A1 and GpsB (and truncations and mutations thereof) fused to the T18 or the T25 fragment of the *Bordetella pertussis* adenylate cyclase were co-transformed in *E. coli* BTH101. Transformants were selected on nutrient agar plates containing ampicillin (100 µg mL^{-1}), kanamycin (50 µg mL^{-1}), X-Gal (0.004%), and IPTG (0.1 mM). The plates were photographed after 40 h of growth at 30°C.

Muropeptide analysis

Analysis of muropeptide profiles was essentially performed as described recently (Rismondo *et al.*, 2015).

Microscopy

Sample aliquots (0.4 µl) from logarithmically growing cultures were spotted onto microscope slides coated with a thin film of agarose (1.5% in distilled water), air-dried and covered with a coverslip. Images were taken with a Nikon Eclipse Ti microscope coupled to a Nikon DS-MBWc CCD camera and processed using the NIS elements AR software package (Nikon).

ACKNOWLEDGEMENTS

This work was financially supported by DFG grants HA 6830/1-1 and HA 6830/1-2 as well as a grant of the FCI (Fonds der chemischen Industrie) to S. H and a BBSRC grant (BB/G015902/1) to W.V. We thank Daniela Vollmer and Jacob Biboy (Newcastle University) for isolation and

analysis of some of the cell wall samples. The authors thank all members of the department for fruitful discussions.

REFERENCES

Allerberger, F. & M. Wagner, (2010) Listeriosis: a resurgent foodborne infection. *Clin Microbiol Infect* **16**: 16-23.

Arnaud, M., A. Chastanet & M. Debarbouille, (2004) New vector for efficient allelic replacement in naturally nontransformable, low-GC-content, gram-positive bacteria. *Appl Environ Microbiol* **70**: 6887-6891.

Aubry, C., C. Goulard, M.A. Nahori, N. Cayet, J. Decalf, M. Sachse, I.G. Boneca, P. Cossart & O. Dussurget, (2011) OatA, a peptidoglycan O-acetyltransferase involved in *Listeria monocytogenes* immune escape, is critical for virulence. *The Journal of infectious diseases* **204**: 731-740.

Bertsche, U., E. Breukink, T. Kast & W. Vollmer, (2005) In vitro murein peptidoglycan synthesis by dimers of the bifunctional transglycosylase-transpeptidase PBP1B from *Escherichia coli*. *J Biol Chem* **280**: 38096-38101.

Biasini, M., S. Bienert, A. Waterhouse, K. Arnold, G. Studer, T. Schmidt, F. Kiefer, T.G. Cassarino, M. Bertoni, L. Bordoli & T. Schwede, (2014) SWISS-MODEL: modelling protein tertiary and quaternary structure using evolutionary information. *Nucleic Acids Res* **42**: W252-258.

Blair, D.E., A.W. Schuttelkopf, J.I. MacRae & D.M. van Aalten, (2005) Structure and metal-dependent mechanism of peptidoglycan deacetylase, a streptococcal virulence factor. *Proc Natl Acad Sci U S A* **102**: 15429-15434.

Boneca, I.G., O. Dussurget, D. Cabanes, M.A. Nahori, S. Sousa, M. Lecuit, E. Psylinakis, V. Bouriotis, J.P. Hugot, M. Giovannini, A. Coyle, J. Bertin, A. Namane, J.C. Rousselle, N. Cayet, M.C. Prevost, V. Balloy, M. Chignard, D.J. Philpott, P. Cossart & S.E. Girardin, (2007) A critical role for peptidoglycan N-deacetylation in *Listeria* evasion from the host innate immune system. *Proc Natl Acad Sci U S A* **104**: 997-1002.

Born, P., E. Breukink & W. Vollmer, (2006) *In vitro* synthesis of cross-linked murein and its attachment to sacculi by PBP1A from *Escherichia coli*. *J Biol Chem* **281**: 26985-26993.

Burke, T.P., A. Loukitcheva, J. Zemansky, R. Wheeler, I.G. Boneca & D.A. Portnoy, (2014) *Listeria monocytogenes* is resistant to lysozyme through the regulation, not the acquisition, of cell wall-modifying enzymes. *J Bacteriol* **196**: 3756-3767.

Claessen, D., R. Emmins, L.W. Hamoen, R.A. Daniel, J. Errington & D.H. Edwards, (2008) Control of the cell elongation-division cycle by shuttling of PBP1 protein in *Bacillus subtilis*. *Mol Microbiol* **68**: 1029-1046.

Cleverley, R.M., J. Rismondo, M.P. Lockhart-Cairns, P.T. Van Bentum, A.J. Egan, W. Vollmer, S. Halbedel, C. Baldock, E. Breukink & R.J. Lewis, (2016) Subunit Arrangement in GpsB, a Regulator of Cell Wall Biosynthesis. *Microbial drug resistance* **22**: 446-460.

Commichau, F.M., F.M. Rothe, C. Herzberg, E. Wagner, D. Hellwig, M. Lehnik-Habrink, E. Hammer, U. Volker & J. Stulke, (2009) Novel activities of glycolytic enzymes in *Bacillus subtilis*: interactions with essential proteins involved in mRNA processing. *Molecular & cellular proteomics : MCP* **8**: 1350-1360.

Cossart, P. & A. Toledo-Arana, (2008) *Listeria monocytogenes*, a unique model in infection biology: an overview. *Microbes Infect* **10**: 1041-1050.

Dutow, P., S.R. Schmidl, M. Ridderbusch & J. Stulke, (2010) Interactions between glycolytic enzymes of *Mycoplasma pneumoniae*. *J Mol Microbiol Biotechnol* **19**: 134-139.

Egan, A.J., R.M. Cleverley, K. Peters, R.J. Lewis & W. Vollmer, (2017) Regulation of bacterial cell wall growth. *FEBS J* **284**: 851-867.

Fleurie, A., S. Manuse, C. Zhao, N. Campo, C. Cluzel, J.P. Lavergne, C. Freton, C. Combet, S. Guiral, B. Soufi, B. Macek, E. Kuru, M.S. VanNieuwenhze, Y.V. Brun, A.M. Di Guilmi, J.P. Claverys, A. Galinier & C. Grangeasse, (2014) Interplay of the serine/threonine-kinase StkP and the paralogs DivIVA and GpsB in pneumococcal cell elongation and division. *PLoS genetics* **10**: e1004275.

Glaser, P., L. Frangeul, C. Buchrieser, C. Rusniok, A. Amend, F. Baquero, P. Berche, H. Bloecker, P. Brandt, T. Chakraborty, A. Charbit, F. Chetouani, E. Couve, A. de Daruvar, P. Dehoux, E. Domann, G. Dominguez-Bernal, E. Duchaud, L. Durant, O. Dussurget, K.D. Entian, H. Fsihi, F. Garcia-del Portillo, P. Garrido, L. Gautier, W. Goebel, N. Gomez-Lopez, T. Hain, J. Hauf, D. Jackson, L.M. Jones, U. Kaerst, J. Kreft, M. Kuhn, F. Kunst, G. Kurapkat, E. Madueno, A. Maitournam, J.M. Vicente, E. Ng, H. Nedjari, G. Nordsiek, S. Novella, B. de Pablos, J.C. Perez-Diaz, R. Purcell, B. Remmel, M. Rose, T. Schlueter, N. Simoes, A. Tierrez, J.A. Vazquez-Boland, H. Voss, J. Wehland & P. Cossart, (2001) Comparative genomics of *Listeria* species. *Science* **294**: 849-852.

Guinane, C.M., P.D. Cotter, R.P. Ross & C. Hill, (2006) Contribution of penicillin-binding protein homologs to antibiotic resistance, cell morphology, and virulence of *Listeria monocytogenes* EGDe. *Antimicrob Agents Chemother* **50**: 2824-2828.

Heijne, G., (1986) The distribution of positively charged residues in bacterial inner membrane proteins correlates with the trans-membrane topology. *EMBO J* **5**: 3021-3027.

Hof, H., (2004) An update on the medical management of listeriosis. *Expert opinion on pharmacotherapy* **5**: 1727-1735.

Hofmann, K. & W. Stoffel, (1993) TMbase - A database of membrane spanning proteins segments. *Biol. Chem. Hoppe-Seyler* **374**: 166.

Karimova, G., J. Pidoux, A. Ullmann & D. Ladant, (1998) A bacterial two-hybrid system based on a reconstituted signal transduction pathway. *Proc Natl Acad Sci U S A* **95**: 5752-5756.

Kawai, Y., R.A. Daniel & J. Errington, (2009) Regulation of cell wall morphogenesis in *Bacillus subtilis* by recruitment of PBP1 to the MreB helix. *Mol Microbiol* **71**: 1131-1144.

Korsak, D., Z. Markiewicz, G.O. Gutkind & J.A. Ayala, (2010) Identification of the full set of *Listeria monocytogenes* penicillin-binding proteins and characterization of PBPD2 (Lmo2812). *BMC Microbiol* **10**: 239.

Land, A.D., H.C. Tsui, O. Kocaoglu, S.A. Vella, S.L. Shaw, S.K. Keen, L.T. Sham, E.E. Carlson & M.E. Winkler, (2013) Requirement of essential Pbp2x and GpsB for septal ring closure in *Streptococcus pneumoniae* D39. *Mol Microbiol* **90**: 939-955.

Lerch-Bader, M., C. Lundin, H. Kim, I. Nilsson & G. von Heijne, (2008) Contribution of positively charged flanking residues to the insertion of transmembrane helices into the endoplasmic reticulum. *Proc Natl Acad Sci U S A* **105**: 4127-4132.

Monk, I.R., C.G. Gahan & C. Hill, (2008) Tools for functional postgenomic analysis of *Listeria monocytogenes*. *Appl Environ Microbiol* **74**: 3921-3934.

Rae, C.S., A. Geissler, P.C. Adamson & D.A. Portnoy, (2011) Mutations of the Listeria monocytogenes peptidoglycan N-deacetylase and O-acetylase result in enhanced lysozyme sensitivity, bacteriolysis, and hyperinduction of innate immune pathways. *Infect Immun* **79**: 3596-3606.

Renier, S., P. Micheau, R. Talon, M. Hebraud & M. Desvaux, (2012) Subcellular localization of extracytoplasmic proteins in monoderm bacteria: rational secretomics-based strategy for genomic and proteomic analyses. *PLoS One* **7**: e42982.

Rismondo, J., J.K. Bender & S. Halbedel, (2017) Suppressor mutations linking *gpsB* with the first committed step of peptidoglycan biosynthesis in *Listeria monocytogenes*. *J Bacteriol* **199**.

Rismondo, J., R.M. Cleverley, H.V. Lane, S. Grosshennig, A. Steglich, L. Möller, G.K. Mannala, T. Hain, R.J. Lewis & S. Halbedel, (2016) Structure of the bacterial cell division determinant GpsB and its interaction with penicillin-binding proteins. *Mol Microbiol* **99**: 978-998.

Rismondo, J., L. Möller, C. Aldridge, J. Gray, W. Vollmer & S. Halbedel, (2015) Discrete and overlapping functions of peptidoglycan synthases in growth, cell division and virulence of *Listeria monocytogenes*. *Mol Microbiol* **95**: 332-351.

Sambrook, J., E.F. Fritsch & T. Maniatis, (1989) *Molecular cloning : a laboratory manual,* p. 3 v. Cold Spring Harbor Laboratory Press, Cold Spring Harbor, N.Y.

655 Sauvage, E., F. Kerff, M. Terrak, J.A. Ayala & P. Charlier, (2008) The penicillin-binding proteins: structure
656 and role in peptidoglycan biosynthesis. *FEMS Microbiol Rev* **32**: 234-258.
657 Swaminathan, B. & P. Gerner-Smidt, (2007) The epidemiology of human listeriosis. *Microbes Infect* **9**:
658 1236-1243.
659 Tavares, J.R., R.F. de Souza, G.L. Meira & F.J. Gueiros-Filho, (2008) Cytological characterization of YpsB, a
660 novel component of the *Bacillus subtilis* divisome. *J Bacteriol* **190**: 7096-7107.
661 Vollmer, W., (2008) Structural variation in the glycan strands of bacterial peptidoglycan. *FEMS Microbiol*
662 *Rev* **32**: 287-306.
663 Vollmer, W., B. Joris, P. Charlier & S. Foster, (2008) Bacterial peptidoglycan (murein) hydrolases. *FEMS*
664 *Microbiol Rev* **32**: 259-286.
665 Vollmer, W. & A. Tomasz, (2000) The *pgdA* gene encodes for a peptidoglycan N-acetylglucosamine
666 deacetylase in Streptococcus pneumoniae. *J Biol Chem* **275**: 20496-20501.
667 Warren, J., A.R. Owen, A. Glanvill, A. Francis, G. Maboni, R.J. Nova, W. Wapenaar, C. Rees & S.
668 Totemeyer, (2015) A new bovine conjunctiva model shows that *Listeria monocytogenes* invasion
669 is associated with lysozyme resistance. *Veterinary microbiology*.
670 Zheng, L., U. Baumann & J.L. Reymond, (2004) An efficient one-step site-directed and site-saturation
671 mutagenesis protocol. *Nucleic Acids Res* **32**: e115.
672 Ziani, W., A.P. Maillard, I. Petit-Hartlein, N. Garnier, S. Crouzy, E. Girard & J. Coves, (2014) The X-ray
673 structure of NccX from *Cupriavidus metallidurans* 31A illustrates potential dangers of detergent
674 solubilization when generating and interpreting crystal structures of membrane proteins. *J Biol*
675 *Chem* **289**: 31160-31172.

676

677

678

679 **FIGURES**

680

681 **Fig. 1:** Lysozyme resistance of *L. monocytogenes gpsB* and *pbpA1* mutant strains.

682 (A) Increased lysozyme resistance in the absence of GpsB. *L. monocytogenes* strains EGD-e (wt),

683 LMJR19 (Δ*gpsB*) and the IPTG-inducible *gpsB* mutant LMS56 (I*gpsB* - this syntax is used

684 throughout the manuscript to denote conditional strains containing a deletion of the chromosomal

685 gene and an IPTG-inducible gene copy at an ectopic site) were cultivated in BHI ± 1 mM IPTG,

686 washed and exposed to lysozyme (2.5 µg/ml final concentration). The decrease in optical density

687 was determined in a spectrophotometer. Average values and standard deviations are shown (n=3).

688 (B) Suppression of the increased lysozyme resistance of the Δ*gpsB* mutant by deletion of *pbpA1*.

689 Strains EGD-e (wt), LMJR19 (Δ*gpsB*), LMS57 (Δ*pbpA1*) and LMJR38 (Δ*gpsB* Δ*pbpA1*) were

690 subjected to the same assay as described for panel A. Average values and standard deviations

691 were calculated from an experiment performed in triplicate. Significance levels relative to wild

692 type are indicated by asterisks (* - $P<0.01$, ** - $P<0.001$). (C) Growth of the strains shown in

693 panel B in BHI broth at 37°C.

694

695 **Fig. 2:** Effect of an enzymatically inactive *pbpA1* mutation on lysozyme resistance.

696 (A) Scheme illustrating domain architecture of PBP A1 and position of the E116A mutation in

697 the glycosyltransferase domain of PBP A1. (B) Micrographs showing complementation activity

698 of *pbpA1-flag* and *pbpA1E116A-flag* alleles. Strains EGD-e (wt), LMS57 (Δ*pbpA1*), LMJR49

699 (I*pbpA1-flag*) and LMJR51 (I*E116A-flag*) were grown in BHI broth containing 1 mM IPTG

700 (where necessary) to mid-exponential growth phase and analyzed by phase contrast microscopy.

701 Scale bar is 5 µm. (C) Lysis of *L. monocytogenes* strains EGD-e (wt), LMJR19 (Δ*gpsB*), LMS57

702 (Δ*pbpA1*), LMJR38 (Δ*gpsB* Δ*pbpA1*), LMJR57 (Δ*gpsB* I*pbpA1E116A-flag*) and LMJR60 (Δ*gpsB*

I*pbpA1-flag*) in the presence of 2.5 µg/ml lysozyme. Strains LMJR57 and LMJR60 were grown with 1 mM IPTG for expression of *pbpA1-flag* alleles. Average values and standard deviations were calculated from three repetitions. Significance levels (red - LMJR60, black LMJR57) relative to wild type are indicated by asterisks (* - $P<0.01$, ** - $P<0.001$).

Fig. 3: Contribution of HMW PBPs to lysozyme resistance of *L. monocytogenes*.
(A) Lysozyme resistance of mutants lacking HMW PBPs. *L. monocytogenes* strains EGD-e (wt), LMS57 (Δ*pbpA1*), LMS64 (Δ*pbpA2*), LMJR27 (I*pbpB1*), LMJR18 (I*pbpB2*) and LMJR41 (Δ*pbpB3*) were cultivated in BHI broth ± 1 mM IPTG, washed and incubated in the presence of 2.5 µg/ml lysozyme. Optical density was monitored in 15 min intervals. The Δ*gpsB* mutant strain LMJR19 was included for comparison. An experiment addressing spontaneous autolysis of the same set of *pbp* mutants in plain buffer was published earlier and demonstrated that depletion of PBP B1 accelerated autolysis (30% OD reduction within two hours), while all other PBPs had no effect (Rismondo *et al.*, 2015). (B) The increased lysozyme resistance of PBP B1-depleted LMJR27 cells is not suppressed by deletion of *pbpA1*. Strains EGD-e (wt), LMS57 (Δ*pbpA1*), LMJR27 (I*pbpB1*) and LMJR81 (Δ*pbpA1* I*pbpB1*) were grown in BHI broth with or without 1 mM IPTG and lysozyme resistance was analyzed as described. Both experiments were performed three times and standard deviations are indicated. Significance levels relative to wild type are indicated by asterisks (* - $P<0.01$, ** - $P<0.001$).

Fig. 4: Contribution of OatA and PgdA to the lysozyme resistant Δ*gpsB* phenotype.
(A) Growth of strains EGD-e (wt), LMJR19 (Δ*gpsB*), LMS167 (Δ*oatA*) and LMS166 (Δ*gpsB* Δ*oatA*) in BHI broth at 37°C. (B) Lysis experiment measuring lysozyme resistance of the same set of strains as in panel A. Standard deviations were calculated from an experiment performed

three times. Significance levels relative to wild type are indicated (# - $P>0.05$, * - $P<0.01$, ** - $P<0.001$). (C) Growth of strains EGD-e (wt), LMJR19 (Δ*gpsB*), LMS163 (Δ*pgdA*) and LMS170 (Δ*pgdA* I*gpsB*) in BHI medium with or without 1 mM IPTG. For efficient depletion of GpsB in strain LMS170, LMS170 was pre-grown in BHI broth with 1 mM IPTG at 37°C overnight, washed and used to inoculate a depletion culture not containing IPTG. At the next day, cells from such a pre-depleted culture were used to inoculate cultures containing or not containing 1 mM IPTG in order to analyze IPTG-dependent growth as shown here. (D) Lysis experiment measuring lysozyme resistance of the same set of strains as in panel C. Standard deviations were calculated from an experiment performed three times. Significance levels relative to wild type are indicated by asterisks (* - $P<0.01$, ** - $P<0.001$). Please note the extended range of the y-axis.

Fig. 5: Muropeptide analysis of Δ*gpsB* peptidoglycan by HPLC.

(A) Muropeptide profiles obtained by HPLC analysis. Names of strains are indicated and major muropeptide peaks are numbered. (B) Proposed muropeptide structures, which correspond to the six major peaks labelled in panel A. Abbreviations are G*, glucosamine; G, N-acetylglucosamine; M(r), reduced N-acetylmuramic acid (N-acetylmuramitol); *m*-Dap(NH_2), amidated meso-diaminopimelic acid. The positions of the G and G* residues are not known in the two TetraTri[deAc] isomers (I and II). (C) Relative abundance of peaks 1-6 in the peptidoglycan of the three strains analysed here. Average values and variations were calculated from two independent experiments.

Fig. 6: PgdA is an interaction partner of PBP A1.

(A) Bacterial two hybrid analysis testing the interaction of GpsB and PBP A1 with PgdA. Fields boxed with a dashed blue line represent self-interactions, red-boxed fields are interactions

between the three proteins. Empty pUT18 and pKT25 plasmids were included as negative controls. (B) Scheme summarizing all protein-protein interactions observed in the experiment from panel A. (C) Bacterial two hybrid experiment testing truncated variants of PBP A1 (T25 fragments are all connected to the N-terminus of PBP A1 and its truncations) and PgdA (T18 fragments are all fused to the N-terminus of PgdA and its truncated variants) for their ability to interact with each other. Empty pUT18 and pKT25 plasmids were included as negative controls. (D) Model of a possible GpsB/PBP A1/PgdA complex in *L. monocytogenes.* Proteins are drawn schematically according to their domain organization. Abbreviations are as follows: TP - transpeptidase domain, GT - glycosyltransferase domain, C - C-terminal domain, M - middle domain, N - N-terminal domain. The interaction between PBP A1 and GpsB, involving the cytosolic N-terminus of PBP A1 and the lipid binding domain of GpsB, was demonstrated recently (Rismondo *et al.*, 2016).

Fig. 7: Identification of PgdA residues that contribute to the interaction with PBP A1.
(A) Bacterial two hybrid analysis testing the interaction of T25-fusions to PBP A1 and PgdA with T18-fusion to full length PgdA, the PgdA transmembrane domain (PgdAΔNMC) and mutant variants thereof. The T25 and T18 fragment were fused to the cytosolic N-terminus in all PBP A1 and PgdA fusion proteins. PgdA residues that are critical for the interaction with PBP A1 are marked in red, residues only important for PgdA dimerization are colored in blue. (B) Model of the transmembrane domain of *L. monocytogenes* PgdA (residues 3-25) obtained with SWISS MODEL (Biasini *et al.*, 2014) on the nickel-cobalt-cadmium resistance protein NccX from *Cupriavidus metallidurans* as template (Ziani *et al.*, 2014). Residues contributing to PBP A1 binding (red) and PgdA dimerization (blue) are shown. (C) Lysis of *L. monocytogenes* strains with *pgdA* mutations affecting the interaction of PgdA with PBP A1 and interaction of PgdA with

775 itself in the presence of lysozyme. Strains were EGD-e (wt), LMS163 (Δ*pgdA*), LMSW4
776 (*pgdAW5A*), LMSW5 (*pgdAR7A*), LMSW6 (*pgdAL8A*), LMSW7 (*pgdAI15A*) and LMSW8
777 (*pgdAV19A*). Experiments were performed three times and average values and standard
778 deviations are shown. Significant differences compared to wild type are indicated by asterisks (*
779 - $P<0.01$, ** - $P<0.001$).
780

781 **Table 1:** Strains and plasmids used in this study

name	relevant characteristics	source*/ reference
Plasmids		
pMAD	*bla erm bgaB*	(Arnaud *et al.*, 2004)
pUT18	*bla* P_{lac}*-cya(T18)*	(Karimova *et al.*, 1998)
pUT18C	*bla* P_{lac}*-cya(T18)*	(Karimova *et al.*, 1998)
pKT25	*kan* P_{lac}*-cya(T25)*	(Karimova *et al.*, 1998)
p25-N	*kan* P_{lac}*-cya(T25)*	(Claessen *et al.*, 2008)
pJR24	*bla erm bgaB* Δ*lmo0441*	(Rismondo *et al.*, 2015)
pJR33	P_{help}*-lacO-pbpA1-flag lacI neo*	(Rismondo *et al.*, 2016)
pJR53	*bla erm bgaB* Δ*pbpA1*	(Rismondo *et al.*, 2015)
pSH226	*bla* P_{lac}*-gpsB-cya(T18)*	(Rismondo *et al.*, 2016)
pSH227	*bla* P_{lac}*-cya(T18)-gpsB*	(Rismondo *et al.*, 2016)
pSH228	*kan* P_{lac}*-cya(T25)-gpsB*	(Rismondo *et al.*, 2016)
pSH229	*kan* P_{lac}*-gpsB-cya(T25)*	(Rismondo *et al.*, 2016)
pSH234	*kan* P_{lac}*-cya(T25)-pbpA1*	(Rismondo *et al.*, 2016)
pSH246	*bla erm bgaB* Δ*gpsB*	(Rismondo *et al.*, 2016)
pJR34	P_{help}*-lacO-pbpA1E116A-flag lacI neo*	this work
pJR140	*bla* P_{lac}*-cya(T18)-pbpA1*	this work
pJR141	*bla* P_{lac}*-cya(T18)-pgdA*	this work
pSH401	*bla erm bgaB* Δ*oatA*	this work
pSH402	*bla erm bgaB* Δ*pgdA*	this work
pSH432	*kan* P_{lac}*-cya(T25)-pgdA*	this work
pSH436	*kan* P_{lac}*-cya(T25)-pbpA1*$^{1-323(\Delta GT)}$	this work
pSH437	*kan* P_{lac}*-cya(T25)-pbpA1*$^{1-91(\Delta GT-TP)}$	this work
pSH438	*bla* P_{lac}*-cya(T18)-pgdA* $^{1-267(\Delta C)}$	this work
pSH439	*bla* P_{lac}*-cya(T18)-pgdA* $^{1-159(\Delta MC)}$	this work
pSH440	*bla* P_{lac}*-cya(T18)-pgdA*$^{1-28(\Delta NMC)}$	this work
pSH448	*bla* P_{lac}*-cya(T18)-pgdA*$^{1-28}$*W5A*	this work
pSH449	*bla* P_{lac}*-cya(T18)-pgdA*$^{1-28}$*I6A*	this work
pSH450	*bla* P_{lac}*-cya(T18)-pgdA*$^{1-28}$*R7A*	this work
pSH451	*bla* P_{lac}*-cya(T18)-pgdA*$^{1-28}$*L8A*	this work
pSH452	*bla* P_{lac}*-cya(T18)-pgdA*$^{1-28}$*S9A*	this work
pSH453	*bla* P_{lac}*-cya(T18)-pgdA*$^{1-28}$*L10A*	this work
pSH454	*bla* P_{lac}*-cya(T18)-pgdA*$^{1-28}$*V11A*	this work
pSH455	*bla* P_{lac}*-cya(T18)-pgdA*$^{1-28}$*I13A*	this work
pSH457	*bla* P_{lac}*-cya(T18)-pgdA*$^{1-28}$*I15A*	this work
pSH458	*bla* P_{lac}*-cya(T18)-pgdA*$^{1-28}$*I16A*	this work
pSH459	*bla* P_{lac}*-cya(T18)-pgdA*$^{1-28}$*V18A*	this work
pSH460	*bla* P_{lac}*-cya(T18)-pgdA*$^{1-28}$*V19A*	this work
pSH461	*bla* P_{lac}*-cya(T18)-pgdA*$^{1-28}$*F20A*	this work
pSH462	*bla* P_{lac}*-cya(T18)-pgdA*$^{1-28}$*I21A*	this work
pSH463	*bla* P_{lac}*-cya(T18)-pgdA*$^{1-28}$*V23A*	this work
pSH464	*bla* P_{lac}*-cya(T18)-pgdA*$^{1-28}$*I24A*	this work
pSH465	*bla* P_{lac}*-cya(T18)-pgdA*$^{1-28}$*F26A*	this work
pSW1	*bla erm bgaB pgdA'*	this work
pSW2	*bla erm bgaB pgdA'* Δ*N*	this work
pSW3	*bla erm bgaB pgdA' I15A*	this work
pSW4	*bla erm bgaB pgdA' W5A*	this work
pSW5	*bla erm bgaB pgdA' R7A*	this work
pSW6	*bla erm bgaB pgdA' L8A*	this work
pSW7	*bla erm bgaB pgdA' V19A*	this work

name	relevant characteristics	source*/ reference
***L. monocytogenes* strains**		
EGD-e	wild-type, serovar 1/2a strain	(Glaser *et al.*, 2001)
LMJR18	Δ*pbpB2* (*lmo2039*) *attB::P_{help}-lacO-pbpB2 lacI neo*	(Rismondo *et al.*, 2015)
LMJR19	Δ*gpsB (lmo1888*)	(Rismondo *et al.*, 2016)
LMJR27	Δ*pbpB1*(*lmo1438*) *attB::P_{help}-lacO-pbpB1 lacI neo*	(Rismondo *et al.*, 2015)
LMJR41	Δ*pbpB3* (*lmo0441*)	(Rismondo *et al.*, 2015)
LMS56	Δ*gpsB attB::P_{help}-lacO-gpsB lacI neo*	(Rismondo *et al.*, 2016)
LMS57	Δ*pbpA1* (*lmo1892*)	(Rismondo *et al.*, 2015)
LMS64	Δ*pbpA2* (*lmo2229*)	(Rismondo *et al.*, 2015)
LMJR21	Δ*pbpA1 attB::P_{help}-lacO-pbpA1 lacI neo*	(Rismondo *et al.*, 2015)
LMJR38	Δ*gpsB* Δ*pbpA1*	(Rismondo *et al.*, 2016)
shg4	Δ*gpsB clpCR254S*	(Rismondo *et al.*, 2017)
shg9	Δ*gpsB murZ$^{1-253}$*	(Rismondo *et al.*, 2017)
LMJR49	Δ*pbpA1 attB::P_{help}-lacO-pbpA1-flag lacI neo*	pJR33 → LMS57
LMJR51	Δ*pbpA1 attB::P_{help}-lacO-pbpA1E116A-flag lacI neo*	pJR34 → LMS57
LMJR57	Δ*gpsB* Δ*pbpA1 attB::P_{help}-lacO-pbpA1E116A-flag lacI neo*	pJR34 → LMJR38
LMJR60	Δ*gpsB* Δ*pbpA1 attB::P_{help}-lacO-pbpA1-flag lacI neo*	pJR33 → LMJR38
LMJR76	Δ*gpsB* Δ*pbpB1 attB::P_{help}-lacO-pbpB1 lacI neo*	pSH246 ↔ LMJR27
LMJR81	Δ*pbpA1* Δ*pbpB1 attB::P_{help}-lacO-pbpB1 lacI neo*	pJR53 ↔ LMJR27
LMJR83	Δ*gpsB* Δ*pbpB3*	pJR24 ↔ LMJR19
LMS163	Δ*pgdA* (*lmo0415*)	pSH401 ↔ EGD-e
LMS166	Δ*gpsB* Δ*oatA*	pSH402 ↔ LMJR19
LMS167	Δ*oatA* (*lmo1291*)	pSH402 ↔ EGD-e
LMS170	Δ*pgdA* Δ*gpsB attB::P_{help}-lacO-gpsB neo*	pSH401 ↔ LMS56
LMS171	Δ*pgdA* Δ*pbpB1 attB::P_{help}-lacO-pbpB1 neo*	pSH401 ↔ LMJR27
LMS172	Δ*oatA* Δ*pbpB1 attB::P_{help}-lacO-pbpB1 neo*	pSH402 ↔ LMJR27
LMSW1	*pgdAΔN*	pSW2 ↔ EGD-e
LMSW4	*pgdAW5A*	pSW4 ↔ LMSW1
LMSW5	*pgdAR7A*	pSW5 ↔ LMSW1
LMSW6	*pgdAL8A*	pSW6 ↔ LMSW1
LMSW7	*pgdAI15A*	pSW3 ↔ LMSW1
LMSW8	*pgdAV19A*	pSW7 ↔ LMSW1

* The arrow (→) stands for a transformation event and the double arrow (↔) indicates gene deletions obtained by chromosomal insertion and subsequent excision of pMAD plasmid derivatives (see experimental procedures for details).

Table 2: Oligonucleotides used in this study.

name	sequence (5′→3′)
JR111	CGGCAGATGCGCGTTTTTATGAACATG
JR112	CGCGCATCTGCCGTTGTTAGAATTGC
SHW553	CGCGCGAGATCTCCACATTTACATTTCGGGTTTCC
SHW554	CGCGCGGTCGACAATTTGGTAAATGCTAGGTAACATG
SHW555	TTTTTACTGCAGCACATTATGCACCTCACCTCAG
SHW556	AATGTGCTGCAGTAAAAATCAGTAGCTAAGATGAGTT
SHW561	GCGCGCGGATCCCCGTCCAATAGCGTGCTGCG
SHW562	GCGCGCCCATGGTCTCGATGCCAATCTATGATC
SHW563	ATTTTGGTCGACTAACTATCCGCCCTTAAGTGGG
SHW564	TAGTTAGTCGACCAAAATAACATCTCCTATTTGTGATAAG
SHW666	GCGCGCTCTAGAGAAAATTAGGTGGATTAGACTTTCAC
SHW667	GCGCGCGGTACCTTCACCATTCTTGAATCTGTTTTG
SHW672	AGGGTACCTAAGTAACTAAGAATTCGGCCG
SHW673	TAGGTACCCTAGCTGTATGAATGGTTAAGCCATC
SHW674	TAGGTACCCTAACTTCTGCGAAAACTTTTCCATC
SHW675	AAGGTACCGAGCTCGAATTCATCG
SHW676	TCGGTACCTTTCGTTTGTTCGTTTTTGCTTTTGGC
SHW677	TCGGTACCTTCAAAGCACCTGTTTCTGCGTCGG
SHW678	TCGGTACCTTTTTTTGGAAACCTATTACACCAATAAAAAC
SHW693	ATTAGGGCGATTAGACTTTCACTAGTTGCCATTC
SHW694	TCTAATCGCCCTAATTTTCTCTAGAGTCGACC
SHW695	AGGTGGGCAAGACTTTCACTAGTTGCCATTC
SHW696	AAGTCTTGCCCACCTAATTTTCTCTAGAGTCG
SHW697	TGGATTGCACTTTCACTAGTTGCCATTCTC
SHW698	TGAAAGTGCAATCCACCTAATTTTCTCTAGAG
SHW699	ATTAGAGCATCACTAGTTGCCATTCTCATTATTG
SHW700	TAGTGATGCTCTAATCCACCTAATTTTCTCTAG
SHW701	AGACTTGCACTAGTTGCCATTCTCATTATTGC
SHW702	AACTAGTGCAAGTCTAATCCACCTAATTTTCTC
SHW703	CTTTCAGCAGTTGCCATTCTCATTATTGCCG
SHW704	GGCAACTGCTGAAAGTCTAATCCACCTAATTTTC
SHW705	TCACTAGCAGCCATTCTCATTATTGCCGTG
SHW706	AATGGCTGCTAGTGAAAGTCTAATCCACCTAATT
SHW707	GTTGCCGCACTCATTATTGCCGTGGTTTTTATTG
SHW708	AATGAGTGCGGCAACTAGTGAAAGTCTAATCC
SHW711	ATTCTCGCAATTGCCGTGGTTTTTATTGGTG
SHW712	GGCAATTGCGAGAATGGCAACTAGTGAAAGTC
SHW713	CTCATTGCAGCCGTGGTTTTTATTGGTGTA
SHW714	CACGGCTGCAATGAGAATGGCAACTAGTGAAAG
SHW715	ATTGCCGCAGTTTTTATTGGTGTAATAGGTTTCC
SHW716	AAAAACTGCGGCAATAATGAGAATGGCAAC
SHW717	GCCGTGGCATTTATTGGTGTAATAGGTTTCCAA
SHW718	AATAAATGCCACGGCAATAATGAGAATGGC
SHW719	GTGGTTGCAATTGGTGTAATAGGTTTCCAAAAAAAG
SHW720	ACCAATTGCAACCACGGCAATAATGAGAATG
SHW721	GTTTTTGCAGGTGTAATAGGTTTCCAAAAAAAGG
SHW722	TACACCTGCAAAAACCACGGCAATAATGAGAATG
SHW723	ATTGGTGCAATAGGTTTCCAAAAAAAGGTACCG

SHW724	ACCTATTGCACCAATAAAAACCACGGCAATAATG
SHW725	GGTGTAGCAGGTTTCCAAAAAAAGGTACCGAG
SHW726	GAAACCTGCTACACCAATAAAAACCACGGC
SHW727	ATAGGTGCACAAAAAAAGGTACCGAGCTCG
SHW728	TTTTTGTGCACCTATTACACCAATAAAAACCAC
SW1	GCGCGCGGATCCTCCACATTTACATTTCGGGTTTCC
SW2	GCGCGCCCATGGTTTGGTTGTACACTTCTTGTGTCGATTG
SW3	CATAATGTCGACCAGAAACAGGTGCTTTGTTAACACTTG
SW4	TTTCTGGTCGACATTATGCACCTCACCTCAGAAAAACC
SW9	TCTAATCGCCCTAATTTTCACATTATGCACCTC
SW10	GAAAGTGCAATCCACCTAATTTTCACATTATG
SW11	TAGTGATGCTCTAATCCACCTAATTTTCACATTATG

787

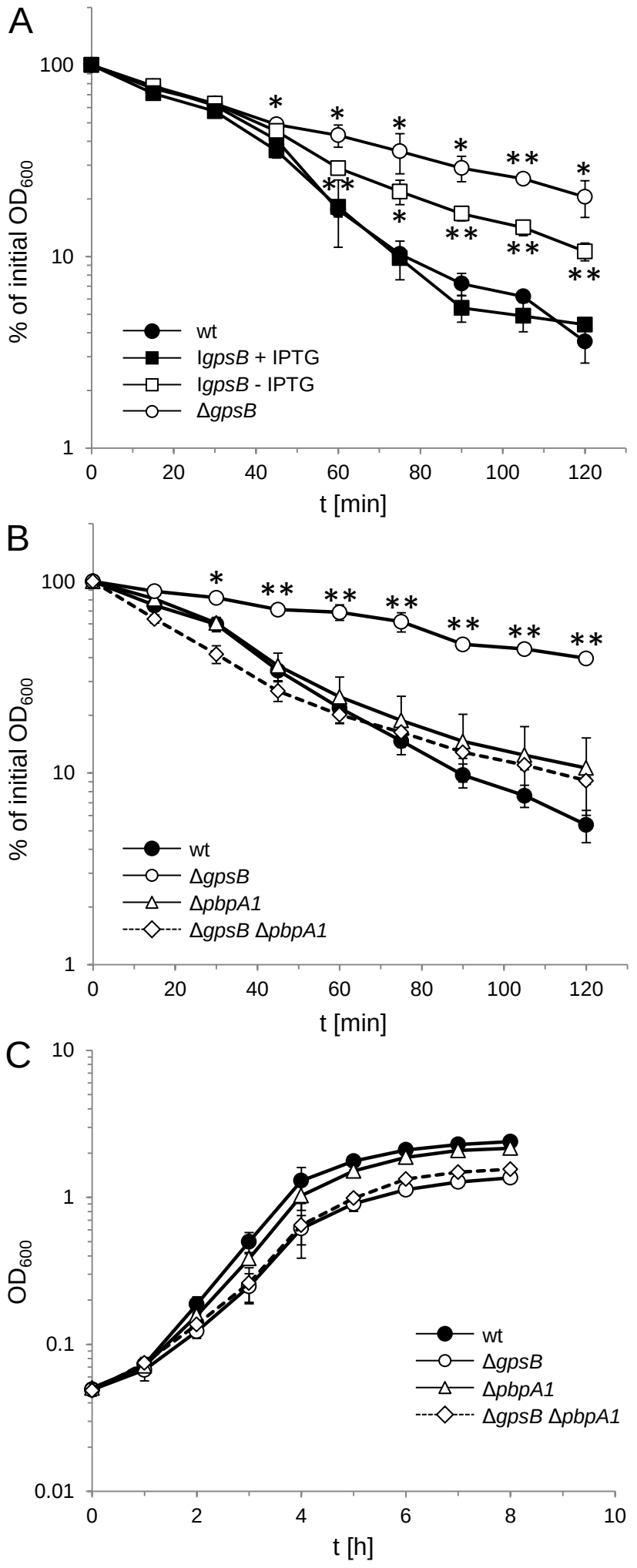

Rismondo *et al.*, Fig. 1

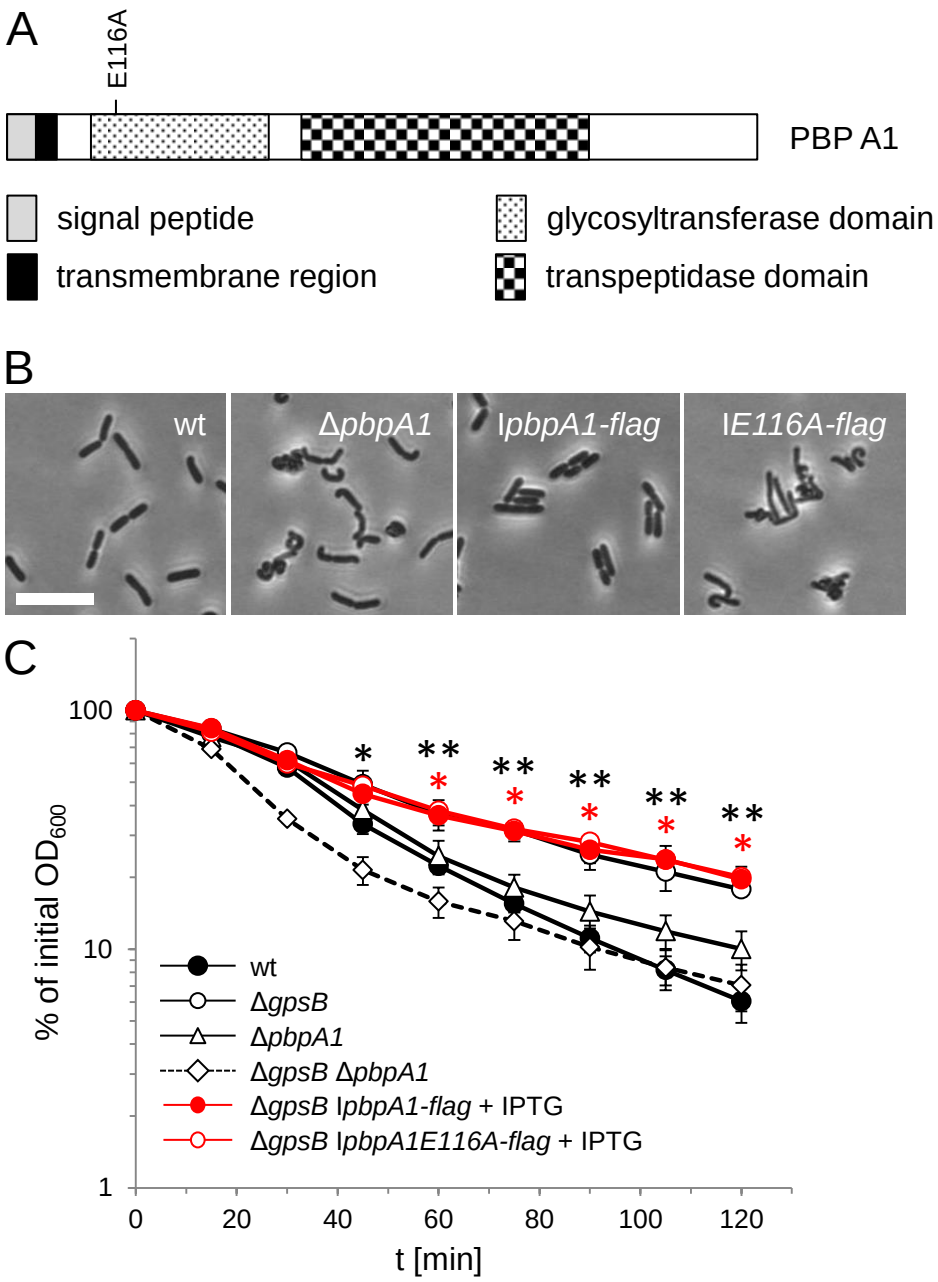

Rismondo *et al.*, Fig. 2

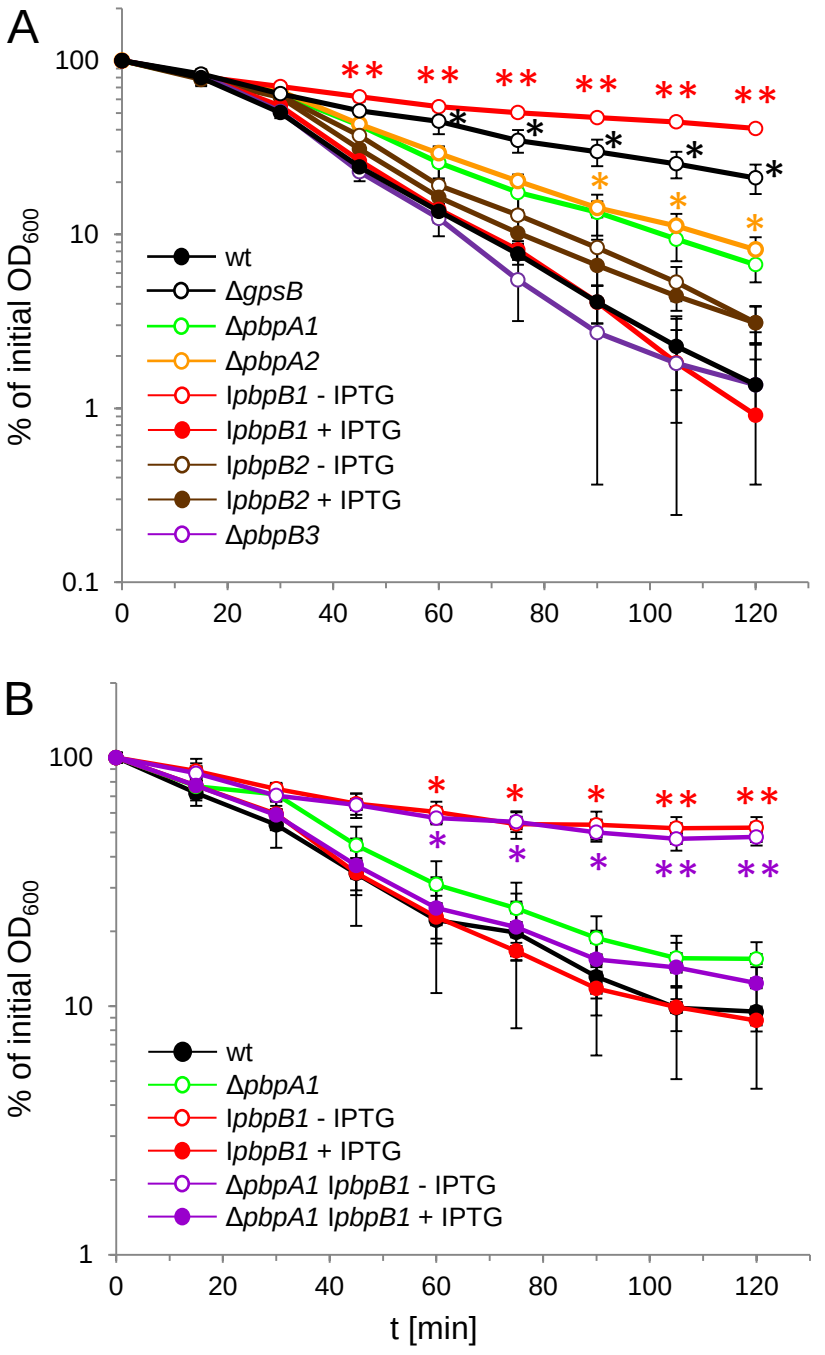

Rismondo *et al.*, Fig. 3

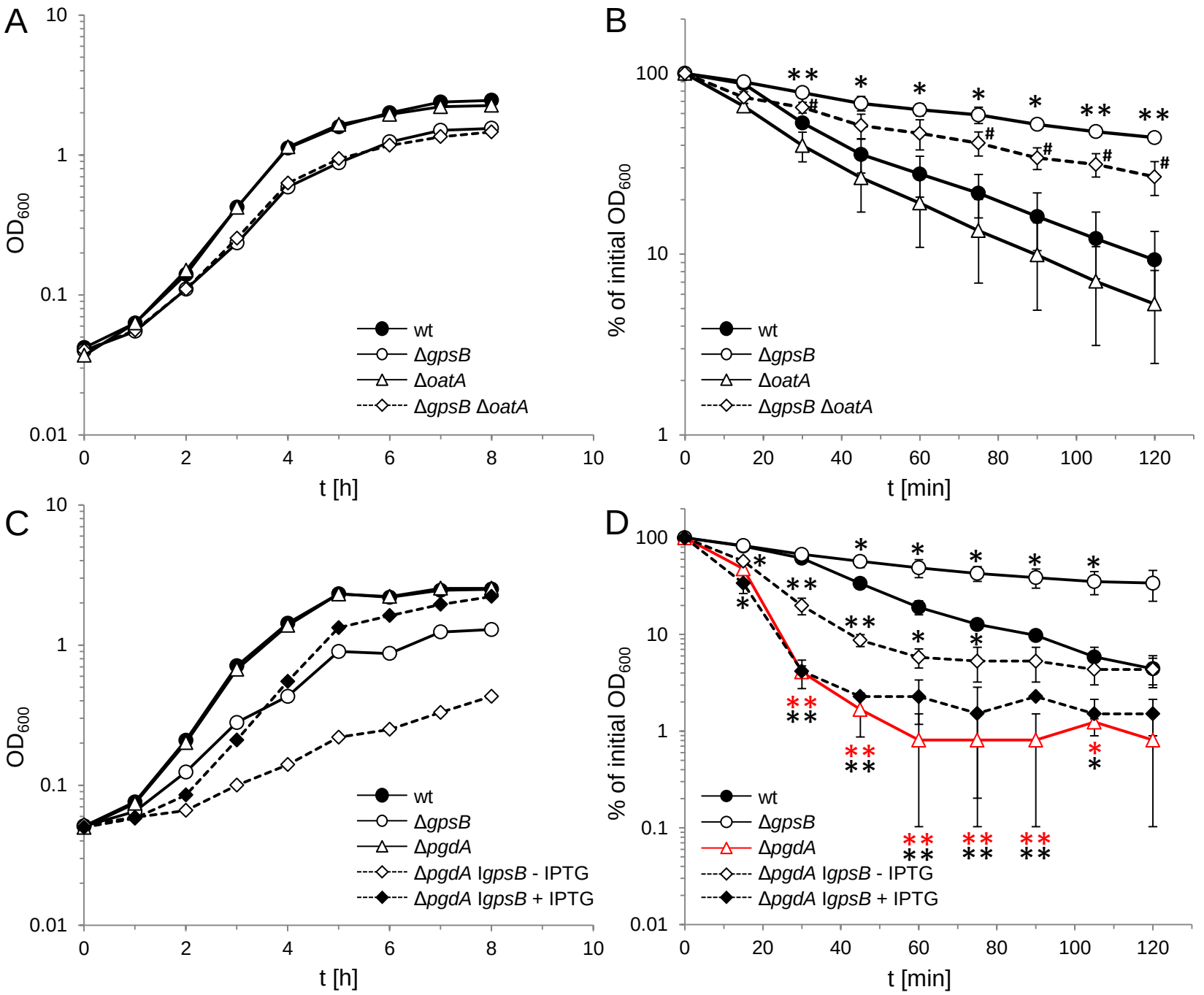

Rismondo *et al.*, Fig. 4

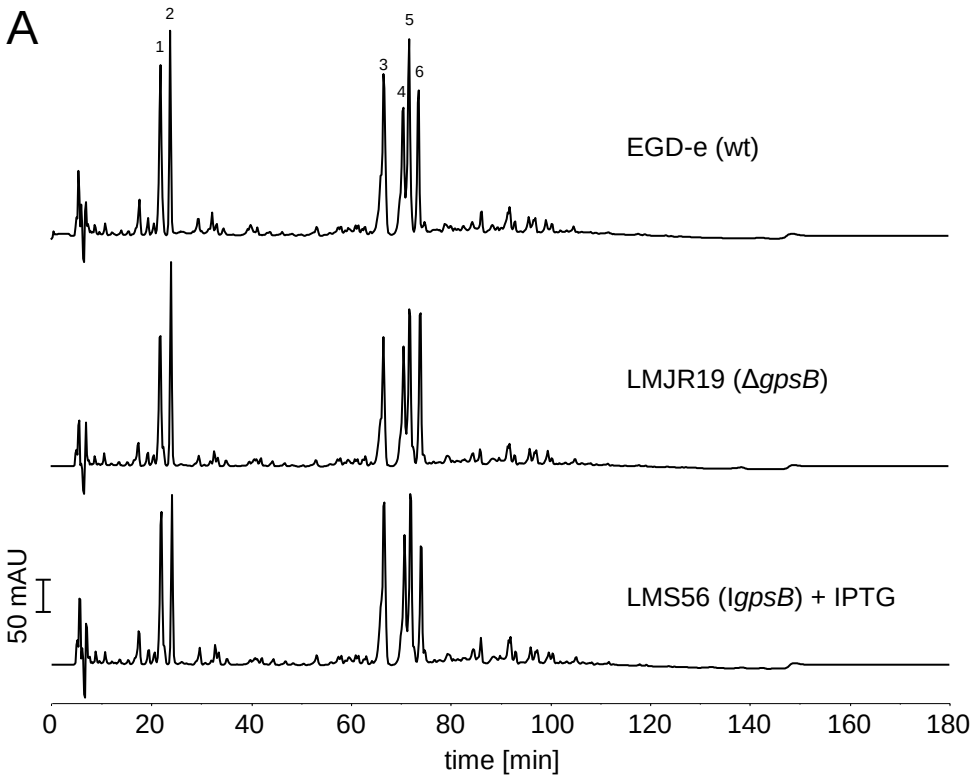

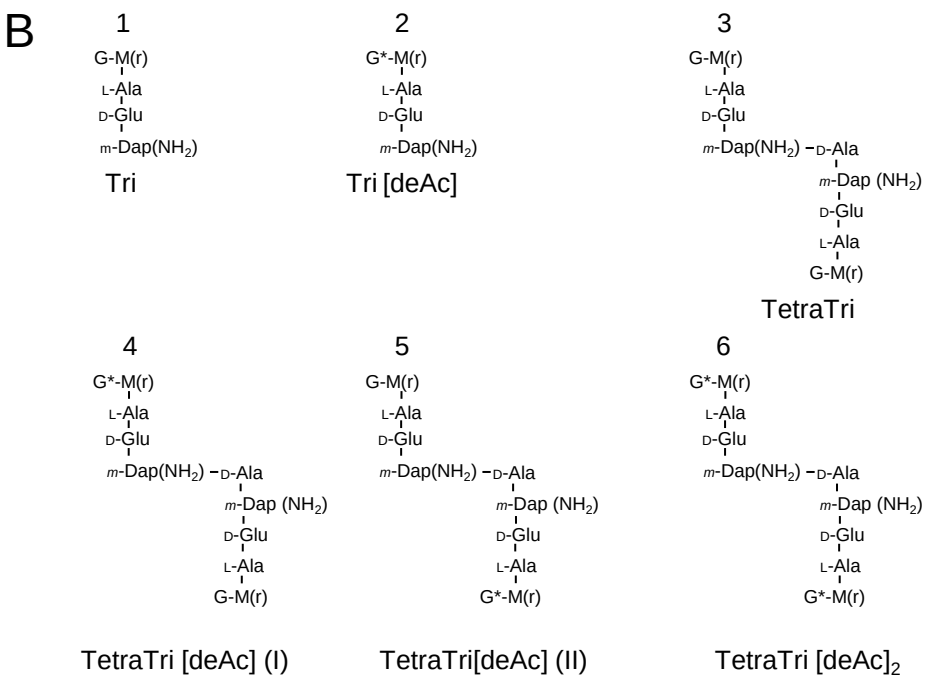

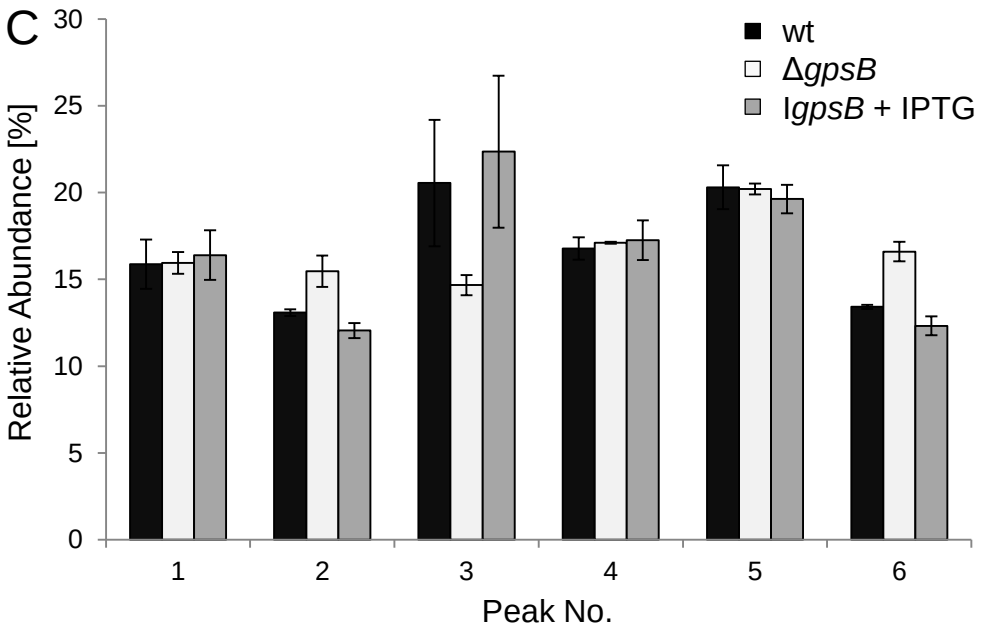

Rismondo *et al.*, Fig. 5

A

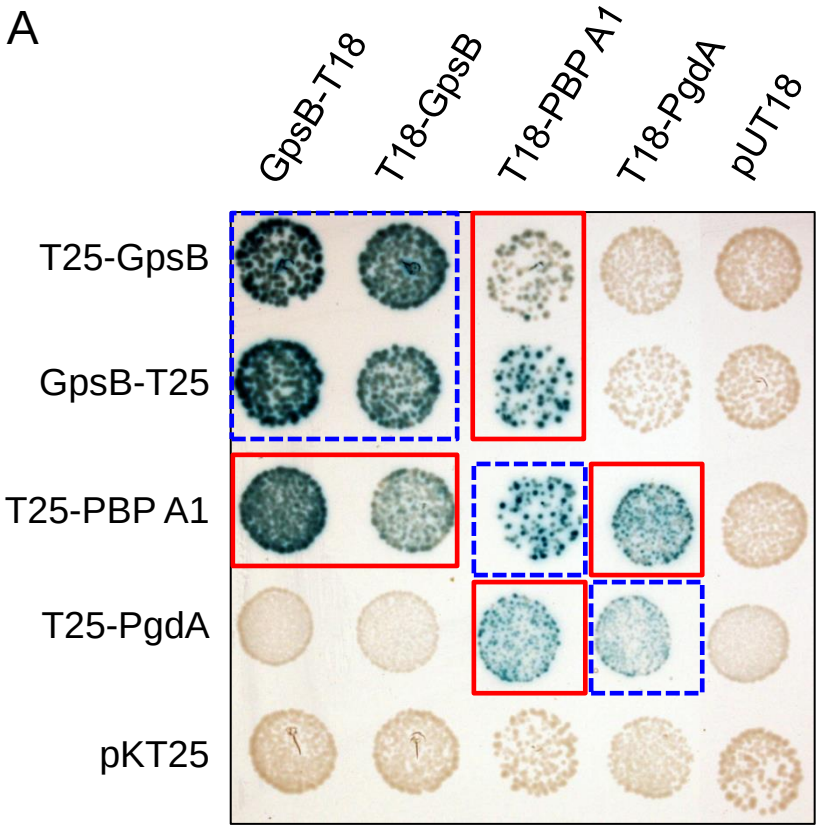

B

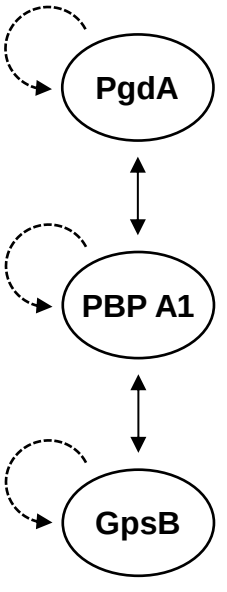

C

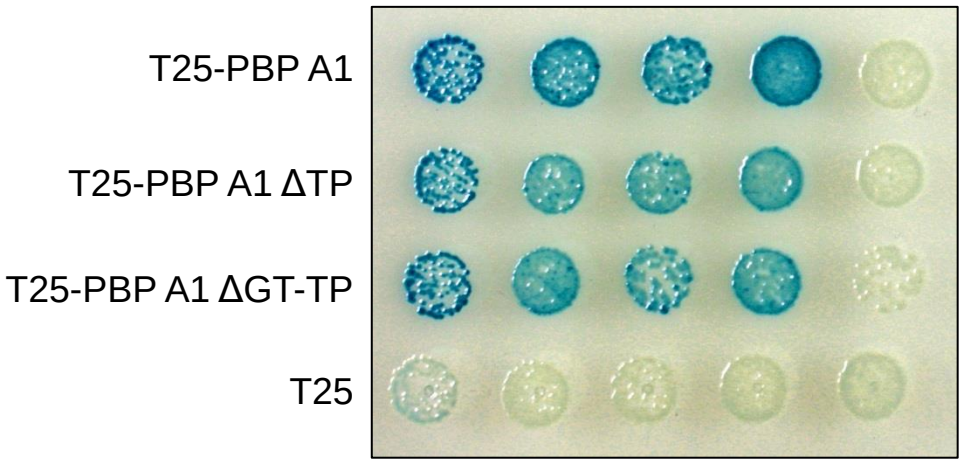

D

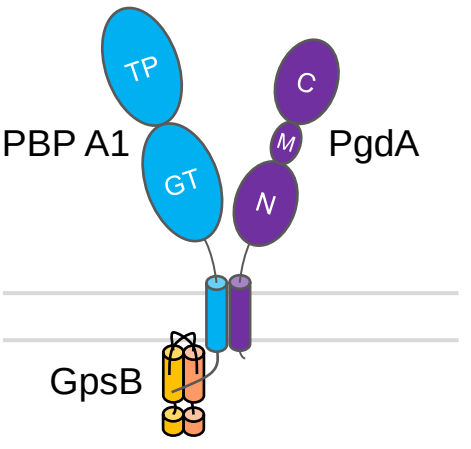

Rismondo *et al.*, Fig. 6

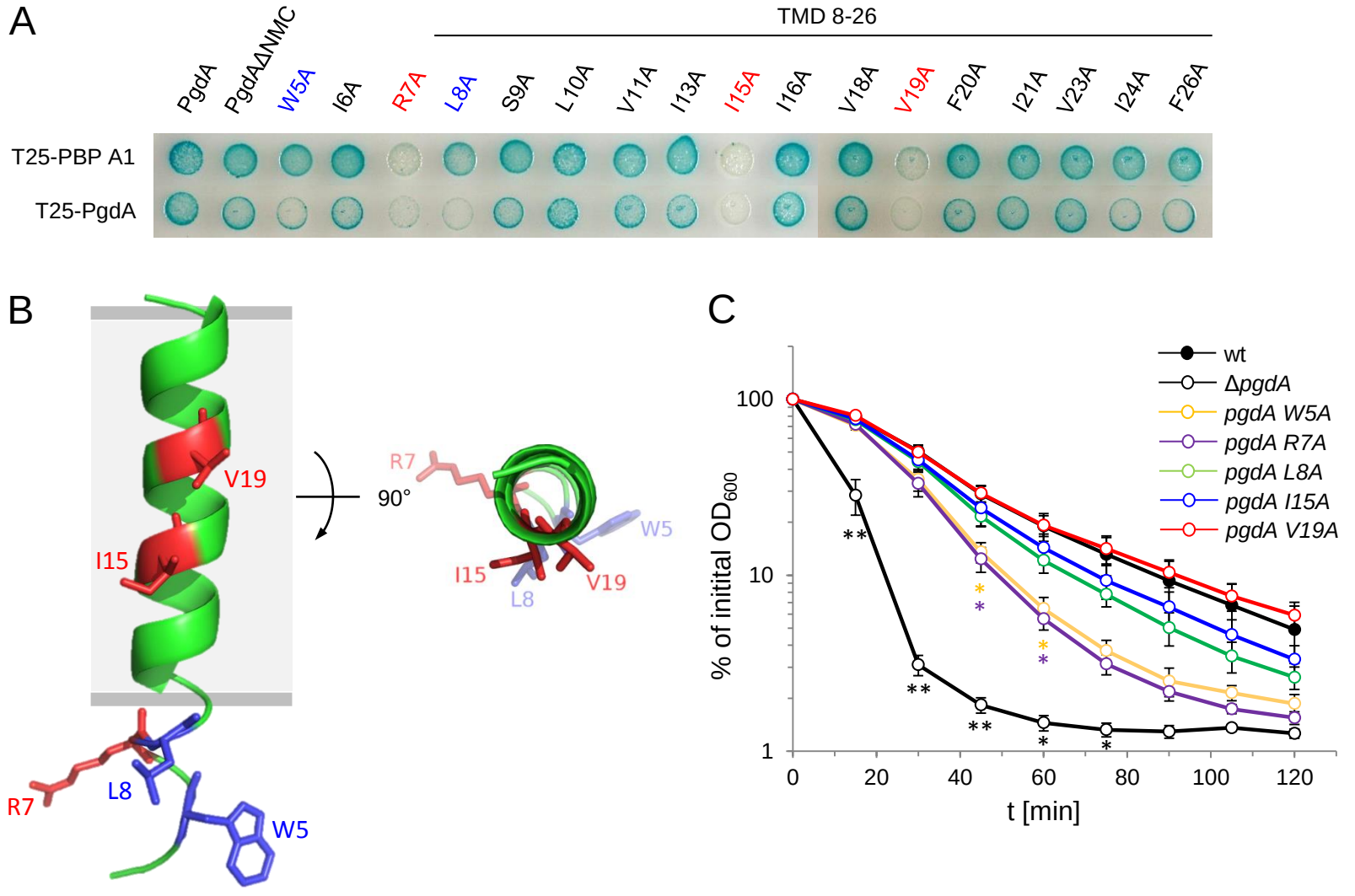

Rismondo *et al.*, Fig. 7

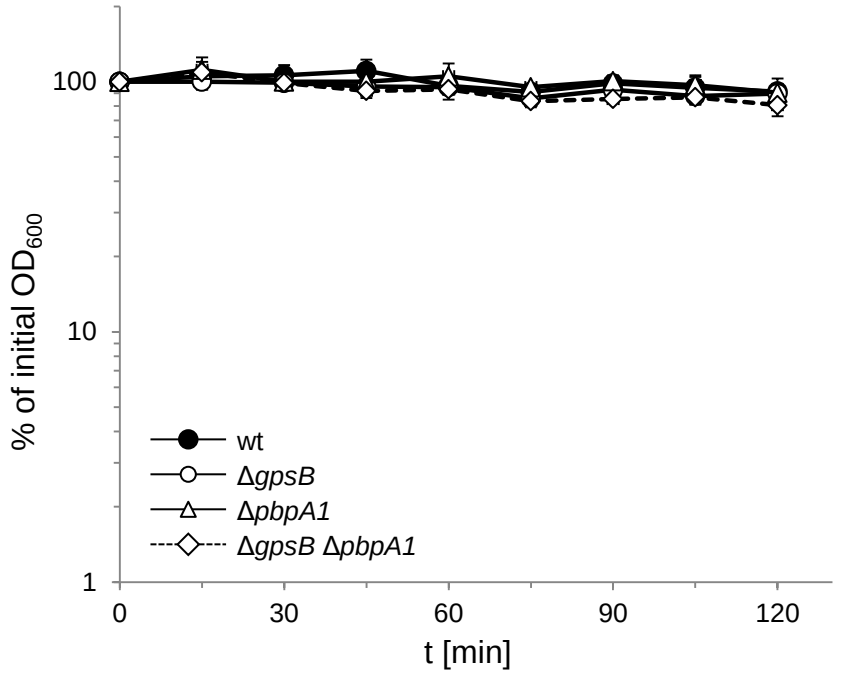

Fig. S1: Spontaneous autolysis of *L. monocytogenes* strains lacking *gpsB* and *pbpA1*.
Cells of *L. monocytogenes* strains EGD-e (wt), LMJR19 (Δ*gpsB*), LMS57 (Δ*pbpA1*) and LMJR38 (Δ*gpsB* Δ*pbpA1*) were grown in BHI broth and resuspended in 50 mM Tris-HCl pH8.0 buffer. Optical density was recorded over time to follow autolysis. Average values and standard deviations were calculated from experiments repeated three times.

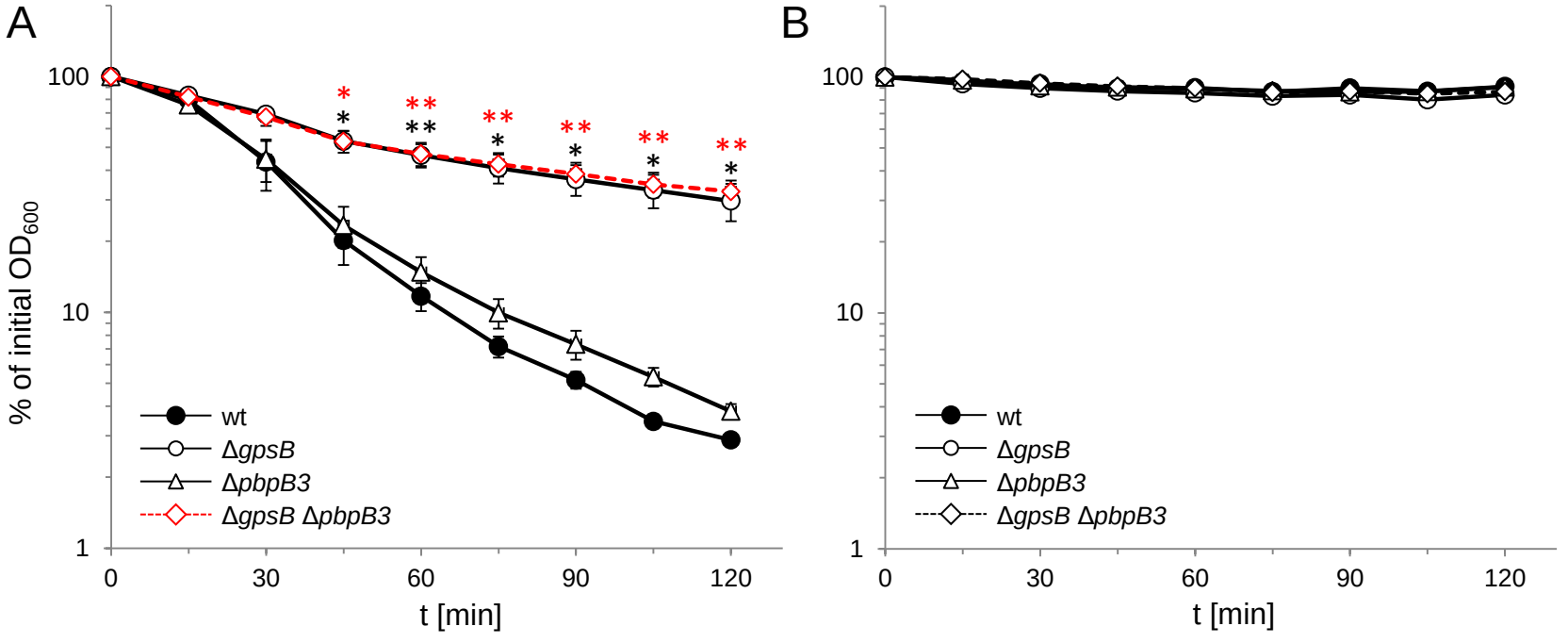

Fig. S2: Effect of PBP B3 on lysozyme resistance of the *L. monocytogenes* Δ*gpsB* mutant.
Cells of *L. monocytogenes* strains EGD-e (wt), LMJR19 (Δ*gpsB*), LMS41 (Δ*pbpb3*) and LMJR83 (Δ*gpsB* Δ*pbpA3*) were grown in BHI broth and resuspended in 50 mM Tris-HCl pH8.0 buffer containing (A) or not containing lysozyme (2.5 µg/ml final concentration, B). Optical density was recorded over time to follow lysozyme-induced lysis (A) and spontaneous autolysis (B). Average values and standard deviations were calculated from experiments repeated three times. Significant differences compared to wild type are indicated by asterisks (* - $P<0.01$, ** - $P<0.001$).

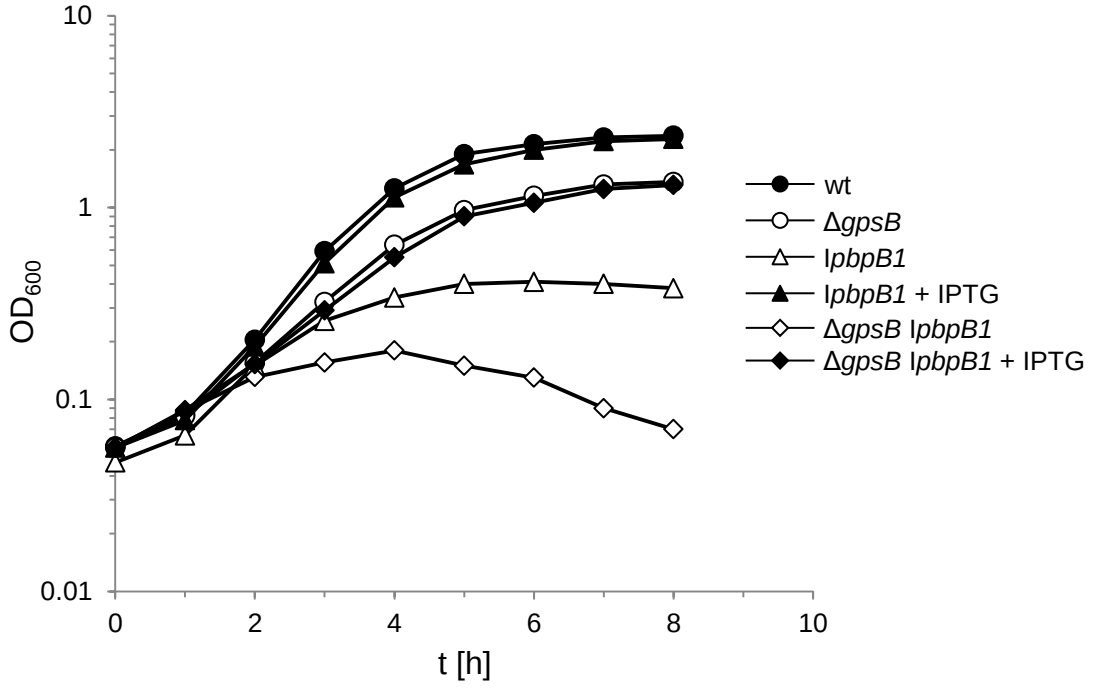

Fig. S3: *L. monocytogenes* does not grow in the absence of *gpsB* and *pbpB1*.
L. monocytogenes strains EGD-e (wt), LMJR19 (Δ*gpsB*), LMJR27 (l*pbpB1*) and LMJR76 (Δ*gpsB* l*pbpB1*) were pregrown in BHI broth (+ 1 mM IPTG where necessary) over night and used to inoculate fresh BHI broth ± 1 mM IPTG the next morning. Cultures were grown at 37°C and growth was recorded in hourly intervals.

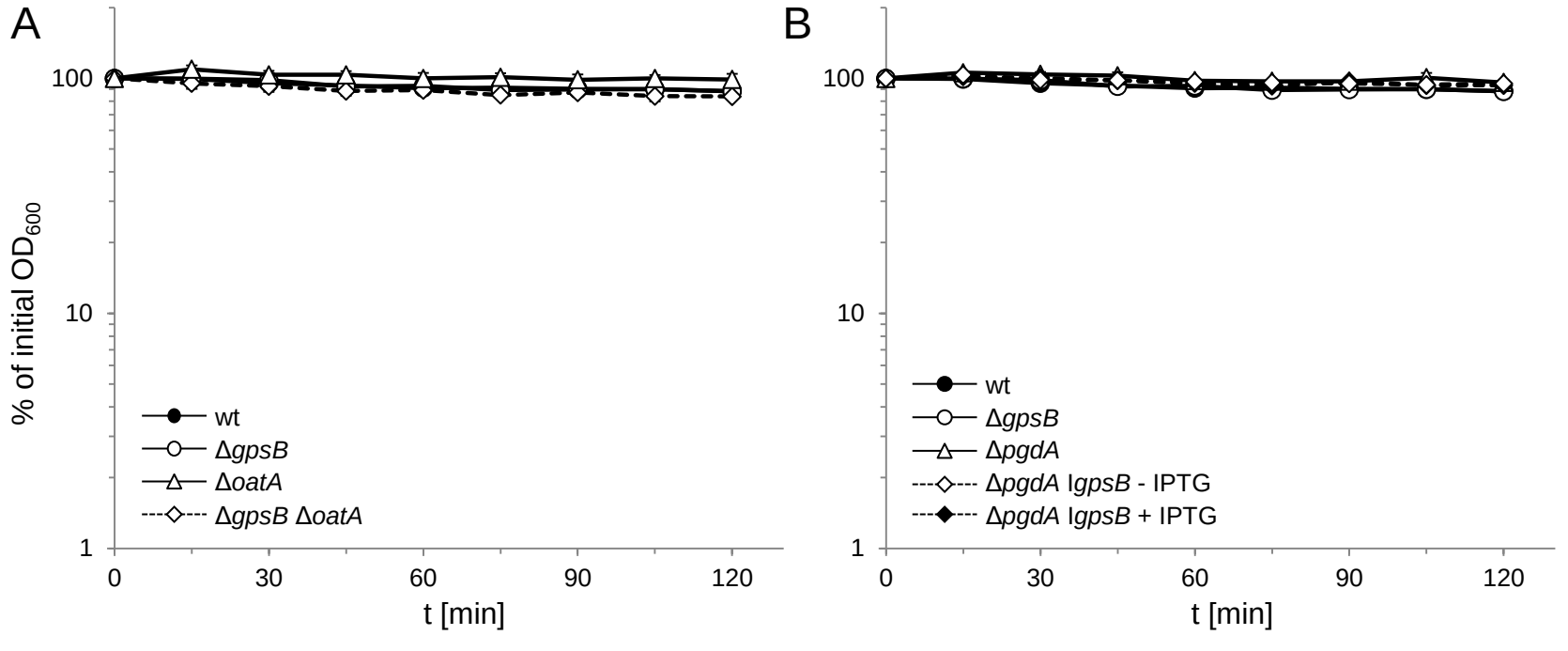

Fig. S4: Spontaneous autolysis *L. monocytogenes gpsB*, *oatA* and *pgdA* mutants.
(A) Effect of *oatA* on spontaneous autolysis of the Δ*gpsB* mutant. Cells of *L. monocytogenes* strains EGD-e (wt), LMJR19 (Δ*gpsB*), LMS167 (Δ*oatA*) and LMS166 (Δ*gpsB* Δ*oatA*) were grown in BHI broth and resuspended in 50 mM Tris-HCl pH8.0 buffer. Optical density was recorded over time to follow autolysis. (B) Effect of *pgdA* on spontaneous autolysis of the GpsB-depleted cells. *L. monocytogenes* strains EGD-e (wt), LMJR19 (Δ*gpsB*), LMS163 (Δ*pgdA*) and LMJR170 (Δ*pgdA* l*gpsB*) were grown in BHI broth ± 1 mM IPTG and resuspended in 50 mM Tris-HCl pH8.0 buffer. Optical density was recorded over time to follow intrinsic autolysis. Average values and standard deviations were calculated from experiments repeated three times.

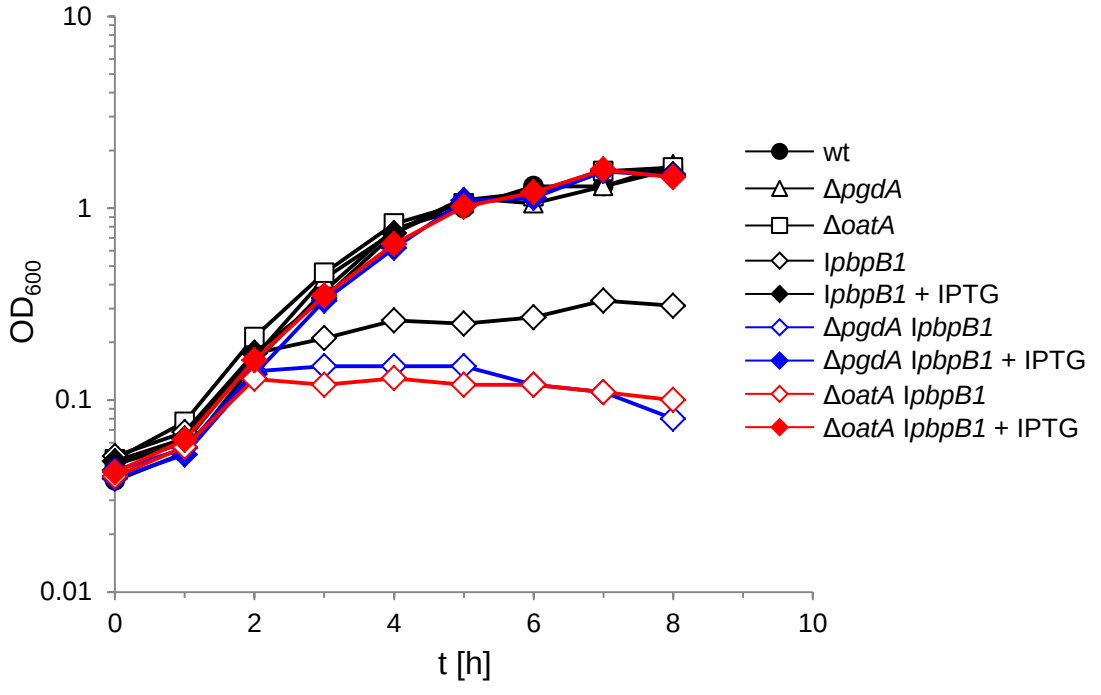

Fig. S5: Increased sensitivity of Δ*pgdA* and Δ*oatA* mutants against depletion of PBP B1.
Growth curves of *L. monocytogenes* strains EGD-e (wt), LMS163 (Δ*pgdA*), LMS167 (Δ*oatA*), LMJR27 (I*pbpB1*), LMS171 (Δ*pgdA* I*pbpB1*) and LMS172 (Δ*oatA* I*pbpB1*) that were grown in BHI broth ± 1 mM IPTG at 37°C.

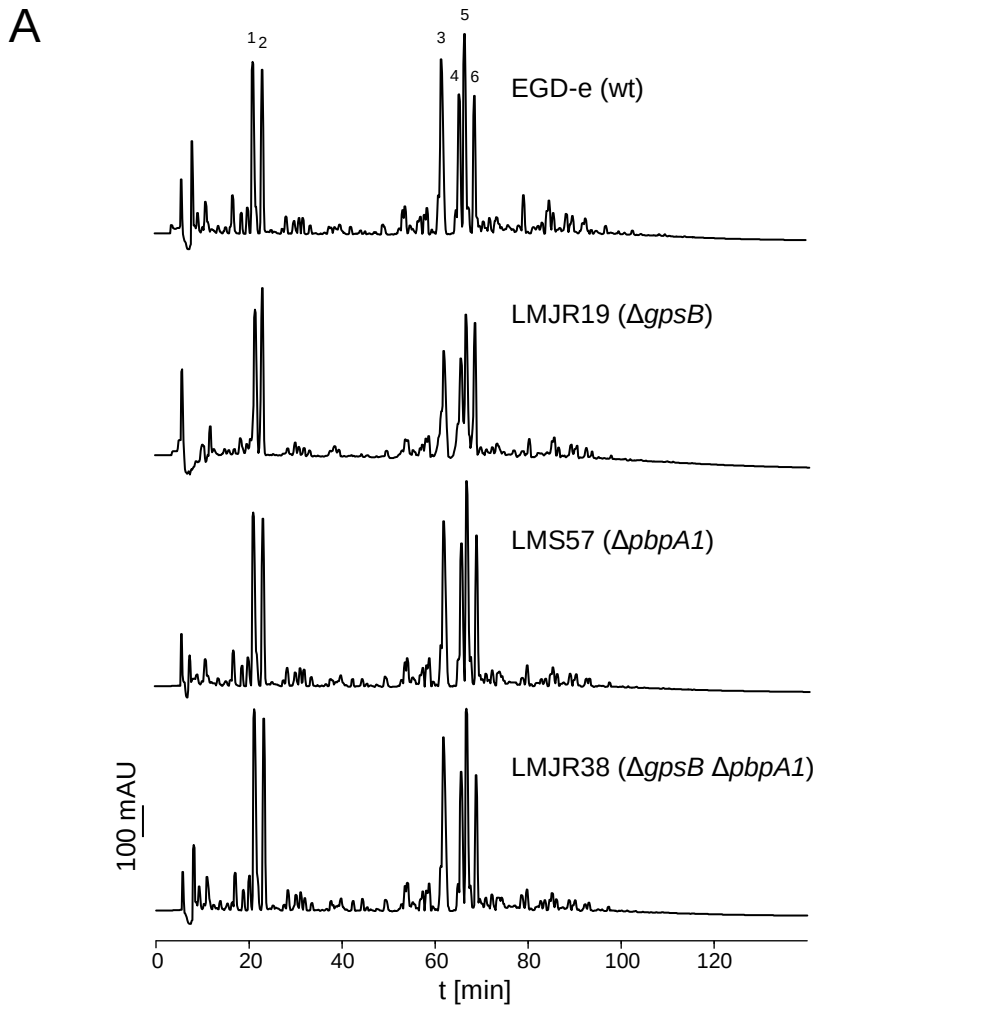

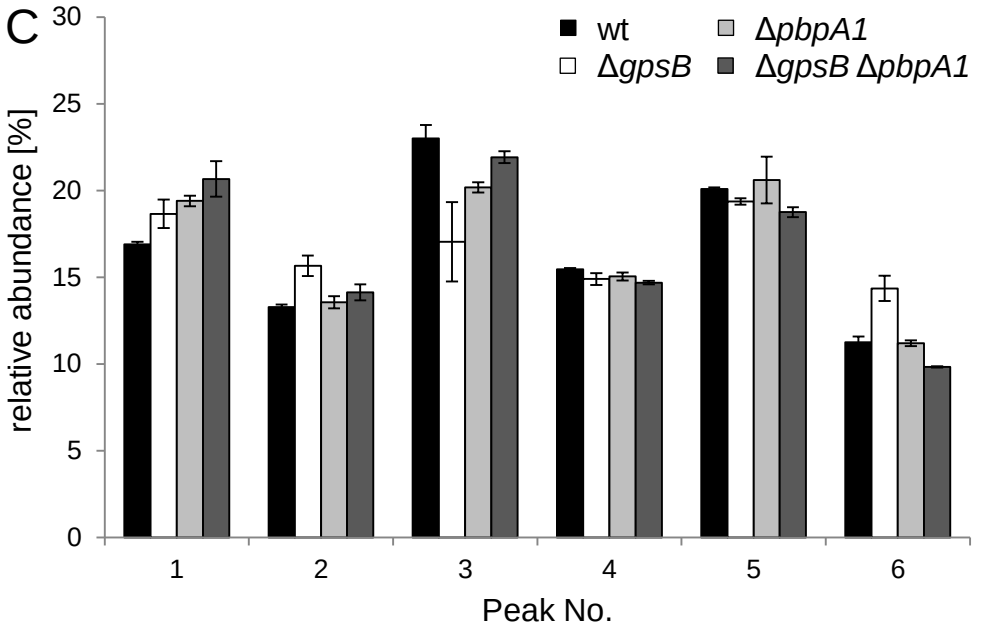

Fig. S6: Muropeptide analysis of Δ*gpsB,* Δ*pbpA1 and* Δ*gpsB* Δ*pbpA1* peptidoglycan by HPLC.
(A) Muropeptide profiles obtained by HPLC analysis. Names of strains are indicated and major muropeptide peaks are numbered. (B) Relative abundance of peaks 1-6 (see Fig. 5B for comparison) in the peptidoglycan of the four strains analysed here. Average values and variations were calculated from two independent experiments.

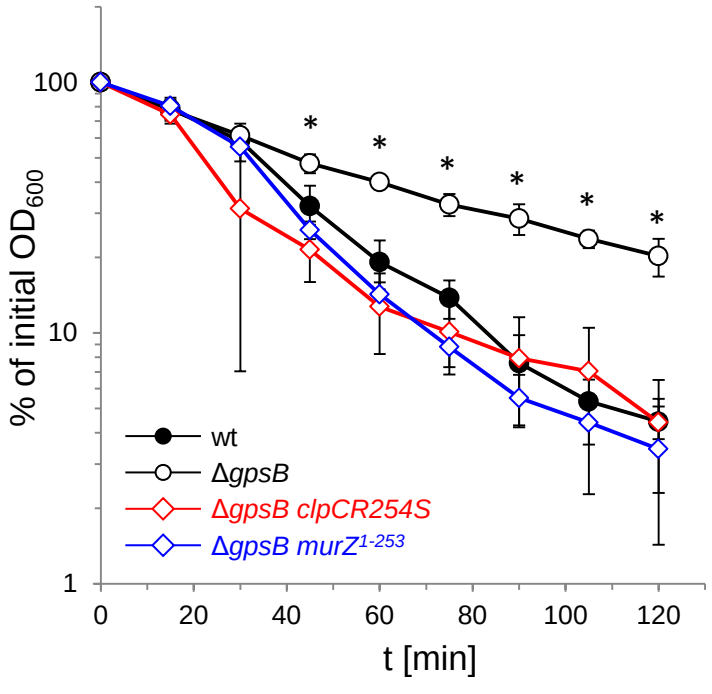

Fig. S7: Sensitivity of *gpsB* suppressor mutants against lysozyme
Lysis of *L. monocytogenes* strains EGD-e (wt), LMJR19 (Δ*gpsB*), *shg4* (Δ*gpsB clpCR254S*) and *shg9* (Δ*gpsB murZ*$^{1–253}$) in the presence of lysozyme. Experiments were performed three times and average values and standard deviations are shown. Significant differences compared to wild type are indicated by asterisks (P<0.01).